Chapter 1

Control design and gain-scheduling using observer-based structures

Daniel Alazard
SUPAERO
10, av. Edouard Belin, 31055 Toulouse, FRANCE
alazard@supaero.fr

1.1 Introduction

Observer-based controllers (for instance Linear Quadratic Gaussian (LQG) controllers) are quite interesting for different practical reasons and from the implementation point of view. Probably the key advantage of these controller structures lies in the fact that the controller states are meaningful variables as estimates of the physical plant states. It follows that the controller states can be used to monitor (on-line or off-line) the performance of the system. Such a meaningful state allows also to initialize the state of the controller or to update controller state during control mode switching. Note that this simple property does not hold for general controllers with state-space description ;

$$\left\{ \begin{array}{rcl} \dot{x}_K & = & A_K x_K + B_K y \\ u & = & C_K x_K + D_K y \, . \end{array} \right. \tag{1.1}$$

Another well-appreciated advantage comes from the ease of implementation of observer-based controllers. In addition to the plant data, only two static gains (the state-feedback gain and the state estimator gain) define the entire controller dynamics. In return, this facilitates the construction of gain-scheduled or interpolated

controllers. Indeed, assuming the plant model is available in real-time, observer-based controllers will only require the storage of these two static gains of lower dimensions instead of the huge set of numerical data in (1.1) to update the controller dynamics at each sample of time. Note that if we are using an interpolating procedure to update the controller dynamics, the general representation in (1.1) is highly questionable from an implementation viewpoint and in many cases will lead to an insuperable computational effort. This was in our opinion a major impediment for a widespread use of modern control techniques such as H_∞ and μ syntheses in realistic applications and particularly for problems necessitating real-time adjustment of the controller gains. These approaches produce high-order controllers expressed under a meaningless state-space realization. Note also that this last point is relevant if a controller reduction has been performed after the design.

To encounter this problem a general procedure is proposed in this chapter to compute an observer based realization for an arbitrary given controller and a given plant (for both continuous and discrete time case). Independently of the solver used for the control design, such a procedure allows to provide a realization with a meaningful state vector. In [1] and [10], it is shown that observer-based realization are also convenient to isolate high level-tuning parameters (potentiometers) in a complex control law. As the observer-based realization exploits the model of the plant, one can also guess that such a realization is very convenient to update the controller to a any change in the model or to built a parameter-dependent controller $K(s,\theta)$ from a parameter-dependent model $G(s,\theta)$.

Among other potential advantages of observer based realization, we would like to point out the possibility to handle actuator saturation constraints by exploiting this information into the prediction equation. Since we do not cover this matter in this document, the reader is referred to [32] and references therein for more details. More theoretical discussions on the implementation of gain-scheduled controllers which exploit information on plant non-linearities are given in [21] and [20].

The practical solution to handle non-stationary problems (like launch vehicle control design during atmospheric flight) or non-linear problems consists in designing a family of controllers at various flight instants or various flight conditions and then in interpolating (gain-scheduling) these various controllers. It is well know that the non-stationary behavior of interpolated control laws depends strongly upon the controller realizations which are interpolated. Observer-based realizations are very attractive from the gain scheduling point of view ([29] and [26]). The main reason is that the controller states are consistent and have physical units if the model on which is built the observer-based realization has physical states. Then, observer-based realizations of given controllers is a good alternative to provide gain-scheduled controllers.

From the control design point of view, the observer-based realization of a controller allows a simple solution to the inverse optimal control problem to be proposed. This solution, called the Cross Standard Form (CSF), is a canonical augmented standard plant whose unique H_∞ or H_2 optimal controller is a given controller. The general idea is to apply the CSF to a given controller in order to set up a standard problem which can be completed to handle frequency-domain H_2 or H_∞ specifications.

In the second section of this chapter, we present the procedure to compute the observer-based realization of a given controller and a given model. The reader will find more details in [3]. The application of this procedure to a very simple missile model is proposed in the third section to illustrate the interest of observer-based controller for gain-scheduling, controller switching and state monitoring. This application has been chosen for its pedagogic feature: demo files can be downloaded on a web page for the reader to run these illustrations on its own personnel computer. In section four, the Cross Standard Form is presented and also applied to the same academic example: a low-order controller is improved to fulfill a template on its frequency-domain response. The extension of theses results to the discrete-time case are gathered in section five. In section six, Cross Standard Form and gain-scheduling using observer-based realizations are applied to the control design for a launch vehicle on the full atmospheric flight envelope. Concluding remarks and future works are proposed in the last section.

Nomenclature

Following notations will be used all along this chapter.

A^T	A transposed
A^+	MOORE-PENROSE pseudo-inverse of matrix A
$A^\perp$	Orthonormal basis for the null space of A
spec(A)	set of eigenvalues for a square matrix A
I_n	$n \times n$ identity matrix
$\mathbb{R}$	set of real numbers
$\mathbb{C}$	set of complex numbers
i	$\sqrt{-1}$
$\dot{x}$	time derivation ($\dot{x} = dx/dt$)
s	LAPLACE variable
LQG	Linear Quadratic Gaussian
$F_l(P, K)$	lower Linear Fractional Transformation of P and K
$\|G(s)\|_2$	H_2 norm of the stable system $G(s)$
$\|G(s)\|_\infty$	H_∞ norm of the stable system $G(s)$
$G(s) := \left[\begin{array}{c\|c} A & B \\ \hline C & D \end{array}\right]$	Shorthand for $G(s) = C(sI - A)^{-1}B + D$

1.2 Observer-based realization of a given controller

In this section, we briefly recall central ideas behind the Youla parameterization and show how it can be used to find the state estimator-state feedback structure of an arbitrary compensator associated with a given plant.

Consider the stabilizable and detectable nth-order system $G(s)$ (m inputs and p outputs) with minimal state-space realization:

$$\left\{ \begin{array}{rcl} \dot{x} & = & Ax + Bu, \\ y & = & Cx + Du \end{array} \right. \tag{1.2}$$

The so-called Youla parameterization of all stabilizing compensators built on the general LQG controller structure is depicted in figure 1.1, where K_c, K_f and $Q(s)$ are respectively the state feedback gain, the state estimator gain and the Youla parameter. The compensator associated with this structure is easily shown to have

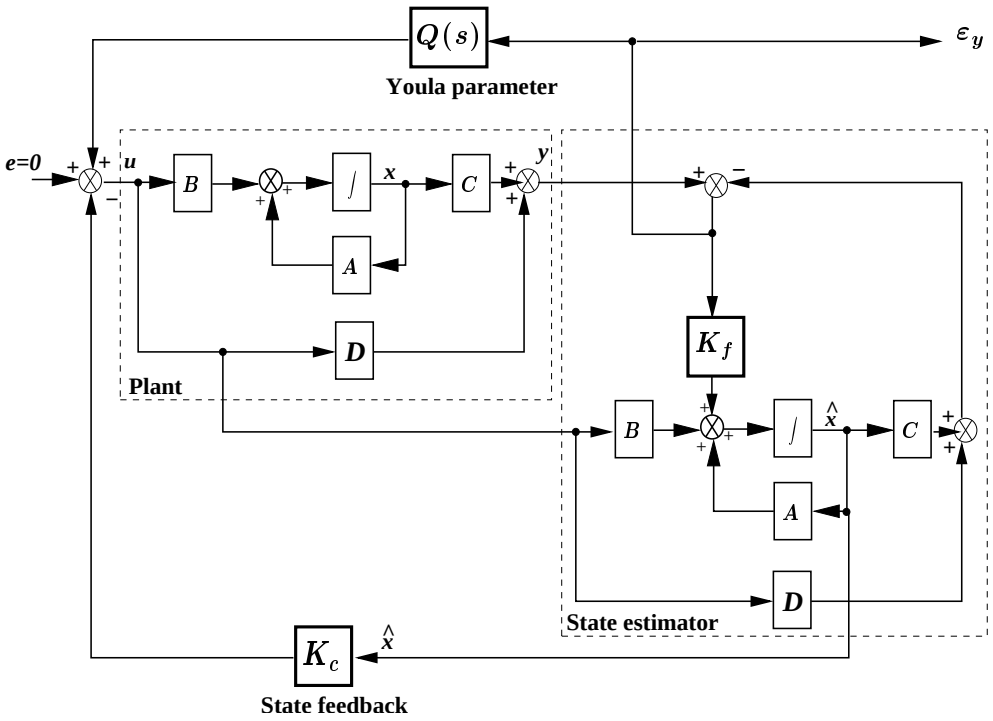

Figure 1.1: Observer-based structure and Youla parameterization.

the following state-space description :

$$\left\{ \begin{array}{rcl} \dot{\widehat{x}} & = & A\widehat{x} + Bu + K_f(y - C\widehat{x} - Du) \\ \dot{x_Q} & = & A_Q x_Q + B_Q(y - C\widehat{x} - Du) \\ u & = & -K_c\widehat{x} + C_Q x_Q + D_Q(y - C\widehat{x} - Du) \end{array} \right. \tag{1.3}$$

where A_Q, B_Q, C_Q and D_Q are the 4 matrices of the state-space representation of $Q(s)$ associated with the state variable x_Q. Hereafter, $\widehat{x}$ denotes an estimate of the plant state x.

The Youla parameterization principle is based on the fact that the closed-loop transfer function between the input e and the innovation $\varepsilon_y = y - C\widehat{x} - Du$ is null (see [23] for instance). As a consequence, changing $Q(s)$ leads to various compensators but the closed-loop transfer function remains unaffected. It is readily shown that this closed-loop transfer function can be represented by the state-space form (1.4)

involving the estimation error $\varepsilon_x = x - \widehat{x}$:

$$\begin{array}{rcl} \begin{bmatrix} \dot{x} \\ \dot{x_Q} \\ \dot{\varepsilon_x} \end{bmatrix} & = & \begin{bmatrix} A - BK_c & BC_Q & BK_c + BD_QC \\ 0 & A_Q & B_QC \\ 0 & 0 & A - K_fC \end{bmatrix} \begin{bmatrix} x \\ x_Q \\ \varepsilon_x \end{bmatrix} + \begin{bmatrix} B \\ 0 \\ 0 \end{bmatrix} e \\ \varepsilon_y & = & \begin{bmatrix} 0 & 0 & C \end{bmatrix} \begin{bmatrix} x \\ x_Q \\ \varepsilon_x \end{bmatrix} \end{array} \tag{1.4}$$

From this representation, the separation principle appears clearly and can be stated in the following terms :

- the closed-loop eigenvalues can be separated into n closed-loop state-feedback poles ($\mathrm{spec}(A - BK_c)$), n closed-loop state-estimator poles ($\mathrm{spec}(A - K_fC)$) and the Youla parameter poles ($\mathrm{spec}(A_Q)$),
- the closed-loop state-estimator poles and the Youla parameter poles are uncontrollable by e,
- the closed-loop state-feedback poles and the Youla parameter poles are unobservable from ε_y. The transfer function from e to ε_y always vanishes.

Now let us consider a stabilizing n_Kth order controller $K_0(s)$ with minimal state-space realization:

$$\left\{ \begin{array}{rcll} \dot{x_K} & = & A_K x_K + B_K y & \text{(a)} \\ u & = & C_K x_K + D_K y & \text{(b)} \end{array} \right. \tag{1.5}$$

In the sequel, the following notations will be used:

$$\boxed{J_m = (I_m - D_K D)^{-1} \quad \text{and} \quad J_p = (I_p - DD_K)^{-1}\,,} \tag{1.6}$$

with the following properties:

- $J_m D_K = D_K J_p$, $J_p D = D J_m$,
- $I_m + D_K D J_m = J_m$, $I_p + J_p D D_K = J_p$.

We are first going to express the compensator state equation (1.5.a) as an Luenberger observer of the variable $z = Tx$. So, we will denote:

$$x_K = \widehat{z} \tag{1.7}$$

According to Luenberger's formulation [23], this problem can be stated as the search of

$$T \in \mathcal{R}^{n_K \times n},\ F \in \mathcal{R}^{n_K \times n_K},\ G \in \mathcal{R}^{n_K \times p}$$

such that

$$\dot{\widehat{z}} = F\widehat{z} + G(y - Du) + TBu \tag{1.8}$$

is an (asymptotic) observer of the variable z, that is $z - \widehat{z}$ vanishes as t goes to infinity. Luenberger has shown that the constraints :

$$TA - FT = GC, \quad \text{and } F \text{ stable} \ , \tag{1.9}$$

ensure that this holds true. Then, with the output equation (1.5.b), the state space representation of the compensator reads :

$$\left\{ \begin{array}{rcl} \dot{\widehat{z}} & = & \Big(F + (TB - GD)C_K\Big)\widehat{z} + \Big(G(I_p - DD_K) + TBD_K\Big)y \\ u & = & C_K\widehat{z} + D_K y \end{array} \right. \tag{1.10}$$

With (1.7), the identification of (1.10) and (1.5) leads to the algebraic relations:

$$\boxed{\begin{array}{rcll} G & = & (B_K - TBD_K)J_p & (1.11) \\ F & = & A_K + (B_K D - TB)J_m C_K & (1.12) \end{array}}$$

These equations with (1.9) guarantee that we are dealing with an observer-based controller. Note that the stability of F (equation (1.9)) is secured whenever the original controller (1.5) is stabilizing. Indeed from (1.2) and (1.10), a closed-loop state space realization reads :

$$\left[\begin{array}{c} \dot{x} \\ \dot{\widehat{z}} \end{array} \right] = \left[\begin{array}{cc} A + BJ_m D_K C & BJ_m C_K \\ GC + TBJ_m D_K C & F + TBJ_m C_K \end{array} \right] \left[\begin{array}{c} x \\ \widehat{z} \end{array} \right] \tag{1.13}$$

Let us consider the change of state coordinates involving the estimation error $\varepsilon_z = z - \widehat{z}$:

$$\left[\begin{array}{c} x \\ \widehat{z} \end{array} \right] = \mathcal{M} \left[\begin{array}{c} x \\ \varepsilon_z \end{array} \right] \ \text{ with } \ \mathcal{M} = \left[\begin{array}{cc} I_n & 0 \\ T & -I_{n_K} \end{array} \right] \ \text{ and } \ \mathcal{M}^{-1} = \mathcal{M}, \tag{1.14}$$

The new state space realization highlights the separation principle :

$$\left[\begin{array}{c} \dot{x} \\ \dot{\varepsilon_z} \end{array} \right] = \left[\begin{array}{cc} A + BJ_m(D_K C + C_K T) & -BJ_m C_K \\ 0 & F \end{array} \right] \left[\begin{array}{c} x \\ \varepsilon_z \end{array} \right] . \tag{1.15}$$

So the set of $n + n_K$ closed-loop eigenvalues include the n_K eigenvalues of F. Therefore F is stable is the initial controller is stabilizing.

Substituting (1.12) and (1.11) in the first relation in (1.9), we get :

$$\boxed{(A_K + B_K D J_m C_K)T - T(A + B J_m D_K C) - T B J_m C_K T + B_K J_p C = 0\ .} \quad (1.16)$$

So, the problem is reduced to solve in T the generalized non-symmetric and rectangular RICCATI equation (1.16) and next to compute F and G using (1.12) and (1.11) respectively.
Equation (1.16) can also be reformulated as :

$$[-T \quad I] A_{cl} \begin{bmatrix} I \\ T \end{bmatrix} = 0 \quad (1.17)$$

where the characteristic matrix A_{cl} associated with the Riccati equation (1.16) is nothing else than the closed-loop system matrix :

$$A_{cl} := \begin{bmatrix} A + B J_m D_K C & B J_m C_K \\ B_K J_p C & A_K + B_K D J_m C_K \end{bmatrix}. \quad (1.18)$$

The RICCATI equation (1.16) can then be solved by standard invariant subspace techniques which consist in :

- finding a n-dimensional invariant subspace $\mathcal{S} := Range(U)$ of the closed-loop system matrix A_{cl}, that is,
$$A_{cl} U = U \Lambda \quad (1.19)$$
This subspace is associated with a set of n eigenvalues, spec(Λ), among the $n + n_K$ eigenvalues of A_{cl}. Such subspaces are easily computed using SCHUR factorizations or eigenvalue decompositions of the matrix A_{cl}. See [15] for more details.

- partitioning the vectors U which span this subspace conformably to the partitioning in (1.18).
$$U = \begin{bmatrix} U_1 \\ U_2 \end{bmatrix}, \quad U_1 \in \mathcal{R}^{n \times n}. \quad (1.20)$$

- computing the solution :
$$\boxed{T = U_2 U_1^{-1}.} \quad (1.21)$$

Narasimhamurthi and Wu have shown in [25] that the existence of a solution T satisfying (1.16) is guaranteed whenever the eigenvalues of the Hamiltonian matrix A_{cl} are distinct. In proposition 1.2.3, a necessary condition is given for the existence of a solution T. In the general case, however, there are finitely many admissible

subspaces $\mathcal{S}$ and thus many solutions. Each solution corresponds to a particular choice of n eigenvalues among the set of closed-loop eigenvalues of A_{cl}.

Then, given a nth-order plant and a n_Kth-order compensator, one can compute the linear combination $T_{n_K \times n} x$ of the plant states which is estimated by the compensator state. An analogous result is also discussed by Fowell and *al* in [8].

The reader will find in
`http://personnel.supaero.fr/alazard-daniel/demos/demo_obr.html`. an interactive MATLAB function `cor2tfg` to compute the matrices T, F and G from a given controller K_0 and a given plant G.

1.2.1 Augmented-order compensators

In this section, we consider the problem where $n_K \geq n$ and our aim is to find a state-feedback gain K_c, a state-estimator gain K_f and a dynamic Youla parameter $Q(s)$ with order $n_K - n$, such that the observer-based compensator structure in figure 1.1 is equivalent to the original controller (1.5). We will assume that T has been computed by the previous technique according to an admissible choice of n poles among the $n + n_K$ closed-loop poles. Next, F and G can be computed from (1.12) and (1.11).

Let us consider the SCHUR decomposition of A_{cl} used to solve in T the RICCATI equation (1.16):

$$\boxed{A_{cl} = \begin{bmatrix} U_1 & U_3 \\ U_2 & U_4 \end{bmatrix} \begin{bmatrix} \Lambda & * \\ 0 & \Lambda^F \end{bmatrix} \begin{bmatrix} U_1^* & U_2^* \\ U_3^* & U_4^* \end{bmatrix}} \tag{1.22}$$

$\begin{bmatrix} U_1 & U_3 \\ U_2 & U_4 \end{bmatrix}$ is a unitary $(n+n_K) \times (n+n_K))$ matrix with $U_1 \in \mathbb{C}^{n \times n}$, $U_2 \in \mathbb{C}^{n_K \times n}$, $U_3 \in \mathbb{C}^{n \times n_K}$ and $U_4 \in \mathbb{C}^{n_K \times n_K}$.

From equations (1.13) and (1.15), we can write:

$$\begin{bmatrix} A + BJ_m(D_K C + C_K T) & -BJ_m C_K \\ 0 & F \end{bmatrix} = \begin{bmatrix} I_n & 0 \\ T & -I_{n_K} \end{bmatrix} A_{cl} \begin{bmatrix} I_n & 0 \\ T & -I_{n_K} \end{bmatrix}. \tag{1.23}$$

As $T = U_2 U_1^{-1}$, substituting (1.22) in (1.23) one can derive [1]:

$$F = V \Lambda^F V^{-1} \quad \text{with:} \quad \boxed{V = U_2 U_1^{-1} U_3 - U_4}. \tag{1.24}$$

[1] Because $\begin{bmatrix} U_1 & U_3 \\ U_2 & U_4 \end{bmatrix}$ is a unitary, it can be shown that $U_4^* = U_4 - U_2 U_1^{-1} U_3$ and $U_3^* + U_4^* U_2 U_1^{-1} = 0$

Λ^F is a $n_K \times n_K$ upper triangular matrix which can de decomposed by blocks with block sizes $n_K - n$ and n. The adequate decomposition of V and V^{-1} allows to write

$$F = [V_1 \quad V_2] \begin{bmatrix} \Lambda^F_{11} & \Lambda^F_{12} \\ 0 & \Lambda^F_{22} \end{bmatrix} \begin{bmatrix} W_1 \\ W_2 \end{bmatrix} \tag{1.25}$$

with:

$$\boxed{V = [\underbrace{V_1}_{n_K - n} \quad \underbrace{V_2}_{n}] \quad \text{and} \quad V^{-1} = \begin{bmatrix} W_1 \\ W_2 \end{bmatrix} \begin{matrix} \}n_K - n \\ \}n \end{matrix}.} \tag{1.26}$$

Let us perform the change of variable :

$$\widehat{z} = \begin{bmatrix} V_1 & V_2 \end{bmatrix} \begin{bmatrix} w_1 \\ w_2 \end{bmatrix} \tag{1.27}$$

in equations (1.8) and (1.9) and introduce the notations :

$$\begin{bmatrix} \widetilde{G_1} \\ \widetilde{G_2} \end{bmatrix} = \begin{bmatrix} W_1 \\ W_2 \end{bmatrix} G; \quad \begin{bmatrix} \widetilde{T_1} \\ \widetilde{T_2} \end{bmatrix} = \begin{bmatrix} W_1 \\ W_2 \end{bmatrix} T. \tag{1.28}$$

Equations (1.8) and (1.9) then become :

$$\begin{cases} \dot{w_1} = \widetilde{F_{11}} w_1 + \widetilde{F_{12}} w_2 + \widetilde{G_1}(y - Du) + \widetilde{T_1} Bu & \text{(a)} \\ \dot{w_2} = \widetilde{F_{22}} w_2 + \widetilde{G_2}(y - Du) + \widetilde{T_2} Bu & \text{(b)} \end{cases} \tag{1.29}$$

and

$$\begin{cases} \widetilde{T_1} A - \widetilde{F_{11}} \widetilde{T_1} - \widetilde{F_{12}} \widetilde{T_2} = \widetilde{G_1} C & \text{(a)} \\ \widetilde{T_2} A - \widetilde{F_{22}} \widetilde{T_2} = \widetilde{G_2} C & \text{(b)} \end{cases} \tag{1.30}$$

Now, we will assume that the SCHUR decomposition has been performed in such a way that $\widetilde{T_2} = W_2 T$ is non singular (in proposition 1.2.4, a necessary condition for T to be full column rank is given) and we perform the second change of variable :

$$w_2 = \widetilde{T_2} \widehat{x} \tag{1.31}$$

From equations (1.29.b) and (1.30.b), one can derive :

$$\dot{\widehat{x}} = A\widehat{x} + Bu + \widetilde{T_2}^{-1} \widetilde{G_2}(y - C\widehat{x} - Du) \tag{1.32}$$

Using now (1.30.a) and (1.31) to substitute $\widetilde{F_{12}} w_2$ into equation (1.29.a), we get :

$$\dot{w_1} = \widetilde{F_{11}}(w_1 - \widetilde{T_1}\widehat{x}) + \widetilde{G_1}(y - C\widehat{x} - Du) + \widetilde{T_1}(A\widehat{x} + Bu) \tag{1.33}$$

Pre-multiplying equation (1.32) by $\widetilde{T_1}$, subtracting it from equation (1.33) and using the last change of variable :

$$w_1 - \widetilde{T_1}\widehat{x} = x_Q \tag{1.34}$$

we obtain :

$$\dot{x_Q} = \widetilde{F_{11}}x_Q + (\widetilde{G_1} - \widetilde{T_1}\widetilde{T_2}^{-1}\widetilde{G_2})(y - C\widehat{x} - Du) \tag{1.35}$$

From (1.7), (1.27), (1.31) and (1.34), one can easily derive the global linear transformation between the compensator original state x_K and the new states $\widehat{x}$ and x_Q :

$$x_K = \widehat{z} = [V_1 \quad T] \begin{bmatrix} x_Q \\ \widehat{x} \end{bmatrix} \tag{1.36}$$

Then, the compensator output equation (1.5.b) can be expressed as ;

$$u = C_K T\widehat{x} + C_K V_1 x_Q + D_K y \tag{1.37}$$

or :

$$u = J_m\left[(C_K T + D_K C)\widehat{x} + C_K V_1 x_Q + D_K(y - C\widehat{x} - Du)\right] \tag{1.38}$$

The identification of the set of equations (1.32), (1.35) and (1.38) with equation (1.3) provides all the parameters for the observer-based controller structure shown in figure 1.1 :

$$\begin{array}{rcll} K_f & = & \widetilde{T_2}^{-1}\widetilde{G_2} = (W_2T)^{-1}W_2G & (1.39) \\ K_c & = & -J_m(C_KT + D_KC) & (1.40) \\ A_Q & = & \widetilde{F_{11}} = W_1FV_1 & (1.41) \\ B_Q & = & \widetilde{G_1} - \widetilde{T_1}\widetilde{T_2}^{-1}\widetilde{G_2} = W_1[I_{n_K \times n_K} - T(W_2T)^{-1}W_2]G & (1.42) \\ C_Q & = & J_mC_KV_1 & (1.43) \\ D_Q & = & J_mD_K & (1.44) \end{array}$$

Remark 1.2.1 If $\boxed{n_K = n}$, then T is square and the decomposition (1.25) of F is such that $V_2 = I_{n\times n}$ and V_1 is empty. Then equations (1.39)-(1.44) become :

$$\begin{array}{rcll} K_f & = & T^{-1}G = (T^{-1}B_K - BD_K)J_p & (1.45) \\ K_c & = & -J_m(C_KT + D_KC) & (1.46) \\ Q(s) & = & D_Q = J_mD_K & (1.47) \end{array}$$

This result then specializes to those of [7].

1.2.2 Discussion

There is a combinatoric of solutions according to the choice of the partition of the closed-loop eigenvalues, first, in the computation of matrix T, and secondly, in the decomposition of matrix F. Hereafter some rules are proposed to reduce the number of admissible choices.

Proposition 1.2.2 *The n eigenvalues chosen for the computation of the solution T of the* Riccati *equation (1.16) using the invariant subspace approach are the n eigenvalues of the closed-loop state feedback associated with the equivalent observer-based controller, i.e, spec$(A - BK_c)$.*

Proof : From (1.18), (1.19) and (1.20), we have :

$$\begin{bmatrix} A + BJ_mD_KC & BJ_mC_K \\ B_KJ_pC & A_K + B_KDJ_mC_K \end{bmatrix} \begin{bmatrix} I_{n\times n} \\ T \end{bmatrix} = \begin{bmatrix} I_{n\times n} \\ T \end{bmatrix} U_1\Lambda U_1^{-1} \tag{1.48}$$

the first row of this matrix equality reads :

$$A + BJ_m(D_KC + C_KT) = U_1\Lambda U_1^{-1} \tag{1.49}$$

using (1.40), we have :

$$A - BK_c = U_1\Lambda U_1^{-1} \tag{1.50}$$

So, the eigenvalues of Λ are the eigenvalues of $A - BK_c$. As a consequence, the n_K remaining eigenvalues are the Luenberger observer poles (i.e. spec(F), see also equation (1.15)), which are shared, in (1.25), between the $n_K - n$ Youla parameter poles (i.e. spec(A_Q)) and the n closed-loop state estimator poles (i.e. spec$(A - K_fC)$).□

Hereafter, we are considering the set of equations (from (1.18), (1.19) and (1.22)) :

$$\begin{bmatrix} A + BJ_mD_KC & BJ_mC_K \\ B_KJ_pC & A_K + B_KDJ_mC_K \end{bmatrix} \begin{bmatrix} U_1 \\ U_2 \end{bmatrix} = \begin{bmatrix} U_1 \\ U_2 \end{bmatrix} \Lambda \tag{1.51}$$

and we shall give a necessary condition, on the choice of the subspace $\mathcal{S}$, for the existence of a solution T (that is, for U_1 to be invertible).

Proposition 1.2.3 *Consider U_1 and U_2 associated with some n-dimensional invariant subspace $\mathcal{S}$ of A_{cl}. Assume there is some uncontrollable plant eigenvalue which is not in spec$(A_{cl}|S)$ then U_1 is singular. In other words,*

$$if\ \exists\ \lambda\ \notin\ spec(\Lambda)\ s.\ t.\ \lambda\ is\ (A,B)\ uncontrollable,\ then\ U_1\ is\ singular \tag{1.52}$$

Proof : Consider the (A, B)-pair and let λ denote an uncontrollable eigenvalue with associated left-eigenvector u. That is,

$$u^T[A - \lambda I \mid B] = 0 \tag{1.53}$$

then, pre-multiplying (1.51) by $[u^T\ 0]$, we get :

$$u^T[(A + BJ_mD_KC)U_1 + BJ_mC_KU_2] = u^TU_1\Lambda \tag{1.54}$$

From (1.53) and (1.54) it follows that :

$$u^TU_1(\Lambda - \lambda I) = 0 \tag{1.55}$$

So, if $\lambda \notin \text{spec}(\Lambda)$ then $u^TU_1 = 0$, that is U_1 is singular. □

We also have a dual property which concerns the column rank of T (that is, for U_2 to be full column rank). It can be stated as follows.

Proposition 1.2.4 *Consider U_1 and U_2 associated with some n-dimensional invariant subspace $\mathcal{S}$ of A_{cl}. Assume there is some unobservable plant eigenvalue in spec$(A_{cl}|S)$, then U_2 is column rank deficient. In other words,*

$$if\ \exists\, \lambda \in spec(\Lambda)\ s.\ t.\ \lambda\ is\ (A, C)\ unobservable,\ then\ U_2\ is\ column\ rank\ deficient. \tag{1.56}$$

Proof : Omitted for brevity. See proposition 1.2.3. □

Propositions 1.2.3 and 1.2.4 are quite useful when an observer-based realization for H_∞ or μ controllers must be computed from the standard problem augmented with input and output frequency weights (see [3] for more details).

Remark 1.2.5 Among all the admissible choices, the only restriction which can reduce the set of solutions is that complex conjugate pairs of poles cannot be separated if we are seeking state-space representations with real coefficients. Note that such a choice is not always possible. For instance, consider the plant $G(s) = 1/s$ and the compensator $K_0(s) = 2/(s + 2)$, then the computation of the state feedback-state estimator form leads to $Q = 0$, $K_c = 1 + i$ (or $1 - i$) and $K_f = 1 - i$ (resp. $1 + i$). Although the gains K_c and K_f are complex, the transfer function of the controller has real coefficients. It can be easily shown that:

- if n (model order) is even, then a real solution always exists,

- if n is odd, then a real solution T exits if the number of real eigenvalues in spec(A_{cl}) is at least equal to 1 and a real parameterization (K_c, K_f, $Q(s)$) exits (in the case $n_K > n$) if the number of real eigenvalues in spec(A_{cl}) is at least equal to 2.

The following selection rules have proved also useful in practical applications of the method:

- affect the fastest poles to spec(A_Q) in such a way that the Youla parameter acts as a direct feedthrough in the compensator,
- assign to spec($A - BK_c$) the n closed-loop poles which are the "nearest" from the n plant poles in order to respect the dynamic behavior of the physical plant and reduce the state-feedback gains,
- assign fast closed-loop poles to spec($A - K_fC$) to have an efficient state estimator.

1.2.3 In brief

The procedure to compute the observer-based form and the dynamic Youla parameter of a given n_Kth-order compensator associated with a nth-order plant ($n_K \geq n$) can be summarized as follows:

- compute the closed-loop matrix A_{cl} (equations (1.18) and (1.6)) and split up the $n + n_K$ eigenvalues of A_{cl} into 3 auto-conjugate sets :
  - n eigenvalues to be assigned to state feedback dynamics spec($A - BK_c$),
  - $n_K - n$ eigenvalues to be assigned to the YOULA parameter dynamics spec(A_Q),
  - n eigenvalues to be assigned to state estimator dynamics spec($A - K_fC$),
- compute a SCHUR or a diagonal decomposition of A_{cl} (equation (1.22)) such that the eigenvalues are ordered on the diagonal according to the previous choice; that is: spec(Λ) = spec($A - BKc$) and spec(Λ^F) = spec(A_Q) $\cup$ spec($A - KfC$),
- compute T, F and G with equations (1.21), (1.12), (1.11),
- compute V, V_1, V_2, W_1, W_2 with equations (1.24), (1.26),

- compute the sought parameters K_c, K_f, A_Q, B_Q, C_Q and D_Q using (1.39)-(1.44) and (1.6).

The reader will find a demo file (corresponding the example proposed in [3]) and an interactive MATLAB function to compute the observer based realization for a given controller and a given plant in:
`http://personnel.supaero.fr/alazard-daniel/demos/demo_obr.html`.

The help of this function is given below:

```
============================================================
  Observer-Based Realization of a given controller
 ============================================================

  [KC,KF,Q,T] = COR2OBR(PLANT,SYS_K) compute a real Observer
  Based Realization, that is the Youla parameterization
  (defined by Kc, Kf and Q), of a given continuous-time
  controller SYS_K for a given continous-time plant
  PLANT in the case:
   NK (SYS_K order) >= N (PLANT order):

  Remarks: * SYS_K, PLANT and Q are defined as SYSTEM matrices,
           * a real solution may not exit,
           * NQ (order of Q) = NK - N.

  This function plots the map of closed-loop eigenvalues (red x)
  and PLANT open-loop eigenvalues (blue +) in the complex plane.
  Then, the user can choose, in a interactive procedure, the
  closed-loop  eigenvalue distribution between:
   * state feedback dynamics [A-BKc] (blue o),
   * state estimation dynamics [A-KfC] (red o),
   * Youla parameter dynamics (Q)  (green o).

  Uncontrollable eigenvalues are automatically assigned to [A-BKc].
  Unobservable eigenvalues are automatically assigned to [A-KfC].
  (the controller SYS_K is assumed to be minimal).
  Auto-conjugate eigenvalues are assigned together.

  T is the transformation matrix between the old and the new state
  space realizations of the controller:
          X_k = T X_hat.
```

```
[KC,KF,Q,T] = COR2OBR(PLANT,SYS_K,TOL) allows a tolerance TOL
(default: 10^-6) to be taken into account in the unobservable
and uncontrollable subspaces computation.

Reference: D. Alazard and P. Apkarian "Exact observer based structures
for arbitrary compensators" International Journal of Robust and
Non-Linear Control, 1999, n.9, pp 101-118

See also: OBR2COR, COR2TFG
```

1.2.4 Reduced-order compensators case

In the case $n_K < n$ (i.e. $dim(z) < dim(x)$), the observer-based structure shown in Figure (1.1) is no more valid. But an interesting alternative can be derived using a reduced-order estimator.

It is interesting to point out the case where $[T^T \ C^T]$ is a rank n matrix (i.e. $p + n_K \geq n$). Then, a reduced observer-based realization involving an estimate $\widehat{x}$ of the plant state x can be obtained by a linear combination of the compensator state $\widehat{z}$ and the plant output y (see Luenberger [23]) :

$$\widehat{x} = H_1\widehat{z} + H_2(y - Du) \tag{1.57}$$

with the constraint :

$$H_1T + H_2C = I_n \tag{1.58}$$

Then, the separation principle still holds and a Youla parameterization (with a static parameter D_Q) built on such a reduced-order estimator reads :

$$\left\{\begin{array}{rcll} \dot{\widehat{z}} & = & F\widehat{z} + G(y - Du) + TBu & \text{(a)} \\ \widehat{x} & = & H_1\widehat{z} + H_2(y - Du) & \text{(b)} \\ u & = & -K_c\widehat{x} + D_Q(y - C\widehat{x} - Du) & \text{(c)} \end{array}\right. \tag{1.59}$$

$$\left\{\begin{array}{rcl} TA - FT & = & GC \\ H_1T + H_2C & = & I_n \end{array}\right. \tag{1.60}$$

As previously, it can be easily shown that the closed-loop poles, with a compensator defined by equations (1.59) and (1.60), are distributed between the n closed-loop state-feedback poles ($\text{spec}(A - BK_c)$) and the n_K estimator poles ($\text{spec}(F)$). Equations (1.16), (1.12) and (1.11) which respectively provide T, F and G are still

valid. The problem is therefore reduced to compute K_c, H_1, H_2 and D_Q such that (from the identification of (1.59.b) and (1.59.c) with (1.5.b)) :

$$\left\{ \begin{array}{ll} J_m C_K = -(K_c + D_Q C) H_1 & (a) \\ J_m D_K = -(K_c + D_Q C) H_2 + D_Q & (b) \\ H_1 T + H_2 C = I_n & (c) \end{array} \right. \tag{1.61}$$

It is easily deduced that :

$$K_c = -J_m (C_K T + D_K C) \tag{1.62}$$

This is the same equation as (1.40), established in the augmented-order compensator case.

To compute H_1, H_2 and D_Q, the following situations can be considered :

- if $\left[\begin{array}{c} T \\ C \end{array} \right]^{-1}$ exists (which implies that $n_K + p = n$) then :

$$\boxed{[\underbrace{H_1}_{n_K} \quad \underbrace{H_2}_{p}] = \left[\begin{array}{c} T \\ C \end{array} \right]^{-1}} \tag{1.63}$$

  and

$$\left[\begin{array}{c} T \\ C \end{array} \right] [H_1 \quad H_2] = \left[\begin{array}{cc} TH_1 & TH_2 \\ CH_1 & CH_2 \end{array} \right] = \left[\begin{array}{cc} I_{n_K} & 0 \\ 0 & I_p \end{array} \right] \tag{1.64}$$

  Hence, relationships (1.61) are satisfied for any D_Q and we can choose $\boxed{D_Q = 0}$ without loss of generality.

- if $n_K > n - p$, then there are several solutions (H_1, H_2) satisfying (1.61.c), one can choose for example the least norm solution (in order to reduce the control gains) using the pseudo-inverse of matrix $[T^T \; C^T]$:

$$\boxed{\left\{ \begin{array}{rcl} H_1 & = & [T^T T + C^T C]^{-1} T^T \\ H_2 & = & [T^T T + C^T C]^{-1} C^T \end{array} \right.} \tag{1.65}$$

  Then, from (1.61):

$$\boxed{D_Q = (J_m D_K + K_C H_2)(I_p - C H_2)^{-1}) \; .}$$

If $n_K < n - p$, it can only be stated that, in open-loop, the compensator state $\widehat{z}$ is an estimate of the linear combination T of the plant state x, that is, the estimation error $\varepsilon_z = Tx - \widehat{z}$ tends to 0 with the following dynamics :

$$\dot{\varepsilon_z} = (A_K + (B_K D - TB) J_m C_K) \varepsilon_z \tag{1.66}$$

In this case ($n_K < n-p$), the only way round consists in performing a reduction of the plant until the previous technique is applicable. The compensator is then interpreted as an observer-based compensator associated to the reduced plant.

In the next section, the interest of observer-based realizations of given controllers is highlighted through 3 examples: plant state monitoring, controllers switching and smooth gain scheduling on a academic second order missile model.

1.3 Illustrations

The model of a missile between the angle of attack α and the thruster deflection δ can be roughly approximated by the second order transfer function:

$$G(s) = \frac{1}{s^2 - 1}$$

associated with the state-space realization:

$$\left[\begin{array}{c} \dot{\alpha} \\ \ddot{\alpha} \\ \hline \alpha \end{array}\right] = \left[\begin{array}{cc|c} 0 & 1 & 0 \\ 1 & 0 & 1 \\ \hline 1 & 0 & 0 \end{array}\right] \left[\begin{array}{c} \alpha \\ \dot{\alpha} \\ \hline \delta \end{array}\right] \quad . \tag{1.67}$$

Let us consider the following stabilizing controller (positive feedback):

$$K_0(s) = -\frac{s^2 + 27s + 26}{s^2 + 7s + 18} \; .$$

A state space realization (modal canonical form [2]) of this controller reads:

$$\left[\begin{array}{c} \dot{x_1} \\ \dot{x_2} \\ \hline \delta \end{array}\right] = \left[\begin{array}{cc|c} -3.5 & 2.398 & 1.027 \\ -2.398 & -3.5 & -1.5 \\ \hline -17.95 & 1.037 & -1 \end{array}\right] \left[\begin{array}{c} x_1 \\ x_2 \\ \hline \alpha \end{array}\right] \quad . \tag{1.68}$$

In this example the closed-loop dynamics reveals multiple eigenvalues:

$$\mathrm{spec}(A_{cl}) = \{-2, \quad -2, \quad -2, \quad -1\} \; .$$

Then, there exists 2 admissible choices to solve in T the Riccati equation (1.16). The choice $\mathrm{spec}(A - BK_c) = \{-1, \quad -2\}$ and the application of the procedure provides the following parameterization:

$$K_c = [3 \quad 3]; \; K_f = [4 \quad 5]^T; \; Q = -1 \; .$$

[2] Such a canonical form can be easily obtained using the `MATLAB` macro-function `canon`; version `6.5.1`. For later versions, `canon(SYS,'modal')` provides a different state-space realization.

Then, the observer-based realization of $K_0(s)$ reads:

$$\left[\begin{array}{c} \dot{\hat{\alpha}} \\ \ddot{\hat{\alpha}} \\ \hline \delta \end{array}\right] = \left[\begin{array}{cc|c} -4 & 1 & 4 \\ -6 & -3 & 4 \\ \hline -2 & -3 & -1 \end{array}\right] \left[\begin{array}{c} \hat{\alpha} \\ \dot{\hat{\alpha}} \\ \hline \alpha \end{array}\right] \tag{1.69}$$

associated with the estimated state vector $\hat{x} = [\hat{\alpha},\ \dot{\hat{\alpha}}]^T$.

The corresponding MATLAB sequence using functions `cor2obr` and `obr2cor` [3] is:

```
G=pck([0 1;1 0],[0;1],[1 0],0);
cor=tf([-1 -27 -26],[1 7 18]);
[a,b,c,d]=ssdata(canon(cor,'modal'));
K=pck(a,b,c,d);
[Kc,Kf,Q]=cor2obr(G,K)
Kob=obr2cor(G,Kc,Kf,Q)
```

A demo file for the following illustrations is also available at:
`http://personnel.supaero.fr/alazard-daniel/demos/demo_obr.html` .

1.3.1 Illustration 1: plant state monitoring

Figures 1.2 and 1.3 plot the closed-loop state responses (missile and controller states) to initial conditions on missile states ($\alpha(t=0) = 1\,rd$ and $\dot{\alpha}(t=0) = -1\,rd/s$). Figure 1.2 is obtained when the first controller realization (equation (1.68)) is used while Figure 1.3 is obtained with the observer-based realization (equation (1.69)). For both simulations the missile state responses are the same because the initial conditions are the same and the input-output behavior of the controller is independent of its realization. But, one can see in Figure 1.2 that there is no straightforward relation between controller states and missile states (α and $\dot{\alpha}$) while Figure 1.3 highlights that (after the transient response of the state estimator) the controller states of the observer-based realization are good estimate of missile states and can be used to monitor missile states for off-line or in-line analysis (for failure diagnosis purposes, for instance). As the plant state are meaningful variables (α (rd) and $\dot{\alpha}$ (rd/s)), one can also conclude that the state feedback gain K_c has a physical dimension: $K_c = [3.\,rd/rd \quad 3.\,s]$; while the dimension of the various components of realization (1.68) is not defined.

[3] See :`http://personnel.supaero.fr/alazard-daniel/demos/demo_obr.html` .

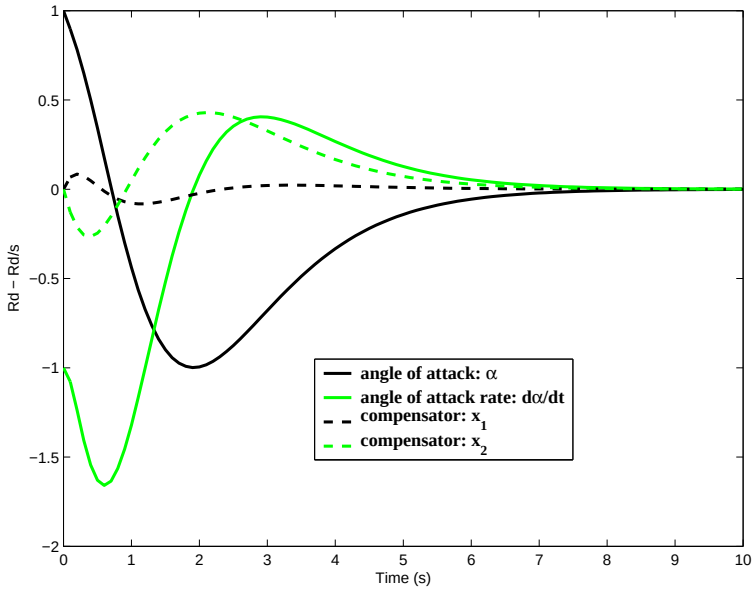

Figure 1.2: Responses to initial conditions on missile states - modal canonical realization of $K_0(s)$ (equation (1.68)).

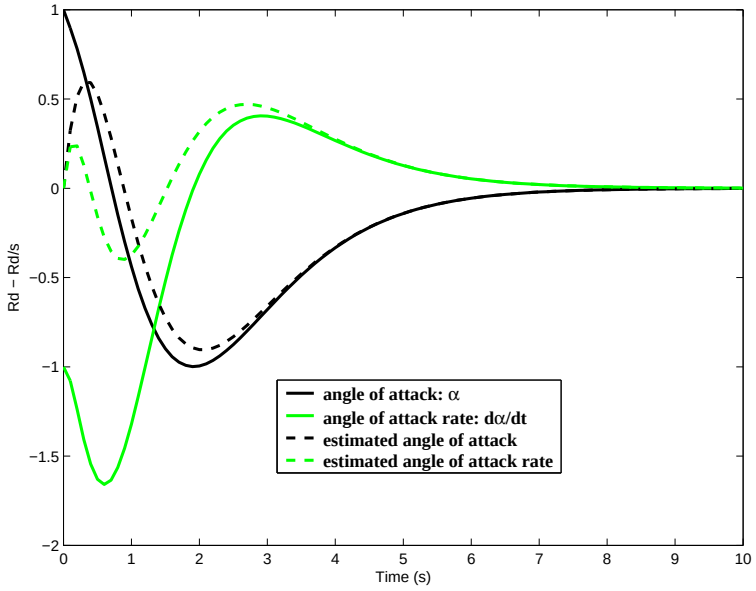

Figure 1.3: Responses to initial conditions on missile states - observer-based realization of $K_0(s)$ (equation (1.69)).

1.3.2 Illustration 2: controllers switching

Let us consider a second stabilizing controller:

$$K_1(s) = -\frac{1667s + 2753}{s^2 + 27s + 353}$$

and let us assume that the control law must switch from controller K_0 to controller K_1 at time $t = 5\,s$. This new controller increases closed-loop dynamic performances required, for instance, during the final flight phase (just before the impact). Indeed, the closed-loop dynamics is now:

$$\text{spec}(A_{cl}) = \{-3, \quad -4, \quad -10 + 10\,i, \quad -10 - 10\,i\}\ .$$

Note that the structure of this new controller K_1 is quite different from the previous one (the direct feed-through term is null in K_1). An observer-based parametrization for $K_1(s)$ reads [4]:

$$K_c = [13 \quad 7];\ K_f = [20 \quad 201]^T;\ Q = 0\ .$$

The state vector initialization of the second controller K_1 with the value of the state vector of the first controller at the switch time ($5\,s$) can create an undesirable transient response (see Figure 1.4 when modal canonical realizations are used for K_0 and K_1). The meaningful state of the observer-based realizations of both controllers allows to initialize correctly the second controller and so allows the transient response on the attitude $\alpha(t)$ to be reduced in a significant way (see Figure 1.5).

1.3.3 Illustration 3: smooth gain scheduling

Now, let us assume that one wishes to interpolate the controller from K_0 to K_1 over $5\,s$. The linear interpolation of the 4 state-space matrices of modal canonical realizations provides a non-stationary controller $K(s,t)$ whose frequency response w.r.t. time t is depicted in Figure 1.6. One can notice that this response is non-monotonous at low frequency and one can also easily check that, at time $2\,s$, the controller $K(s,2)$ does not stabilize the plant $G(s)$.

The interpolation of the 4 state-space matrices of observer-based realizations of K_0 and K_1 provides a smoother interpolation (see Figure 1.7). One can also check that this new interpolated controller stabilizes $G(s)$ for all time $t \in [0,\ 5s]$.

[4] This observer-based parametrization corresponds to the choice affecting the two real closed-loop eigenvalues (i.e. -3 and -4) to the state feedback dynamics).

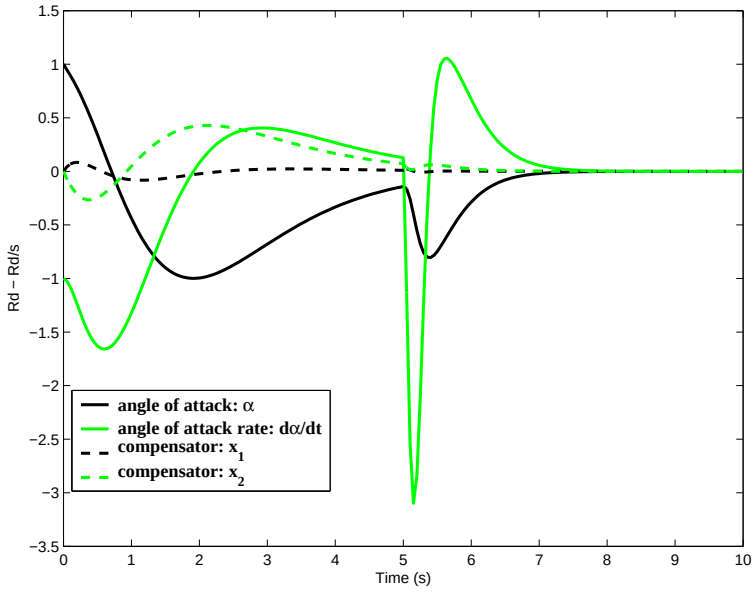

Figure 1.4: Responses to initial conditions and switch from $K_0(s)$ to $K_1(s)$ at time $t = 5\,s$ - modal canonical realizations of $K_i(s)$.

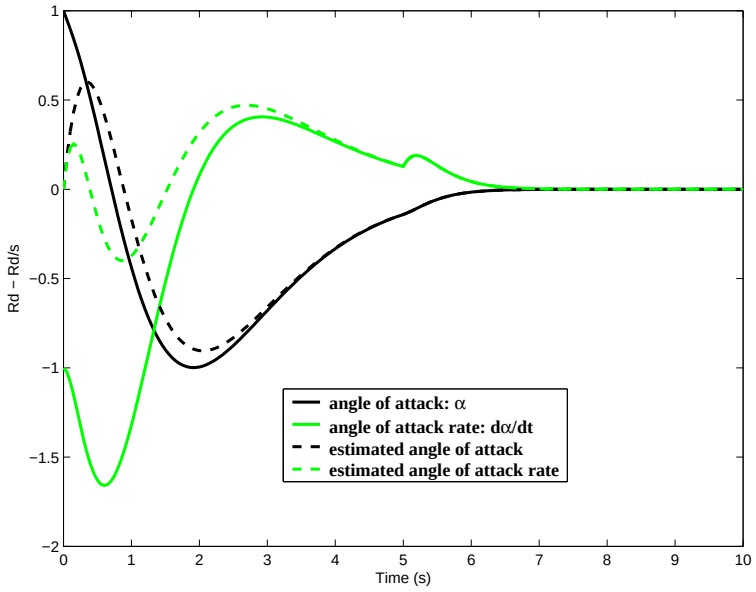

Figure 1.5: Responses to initial conditions and switch from $K_0(s)$ to $K_1(s)$ at time $t = 5\,s$ - observer-based realizations of $K_i(s)$.

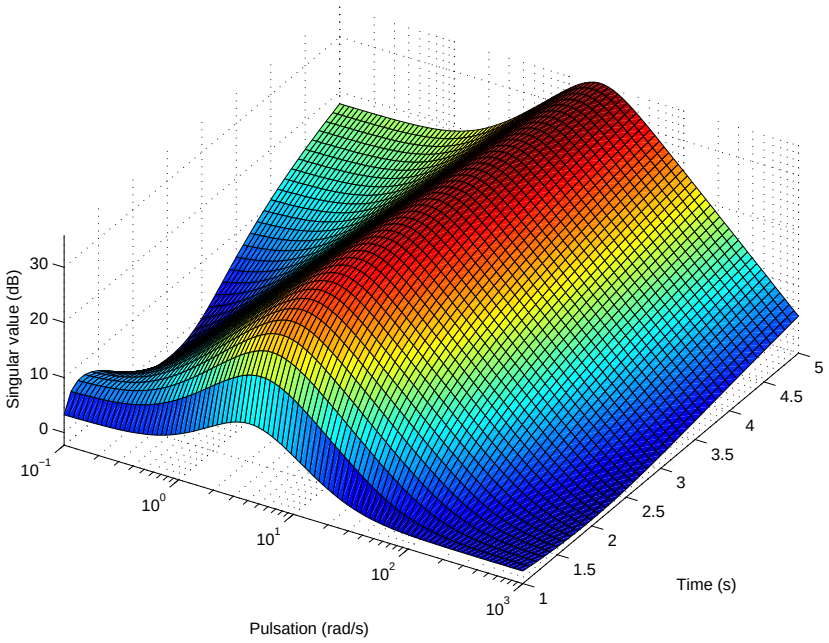

Figure 1.6: $K(s,t)$: singular value w.r.t time.

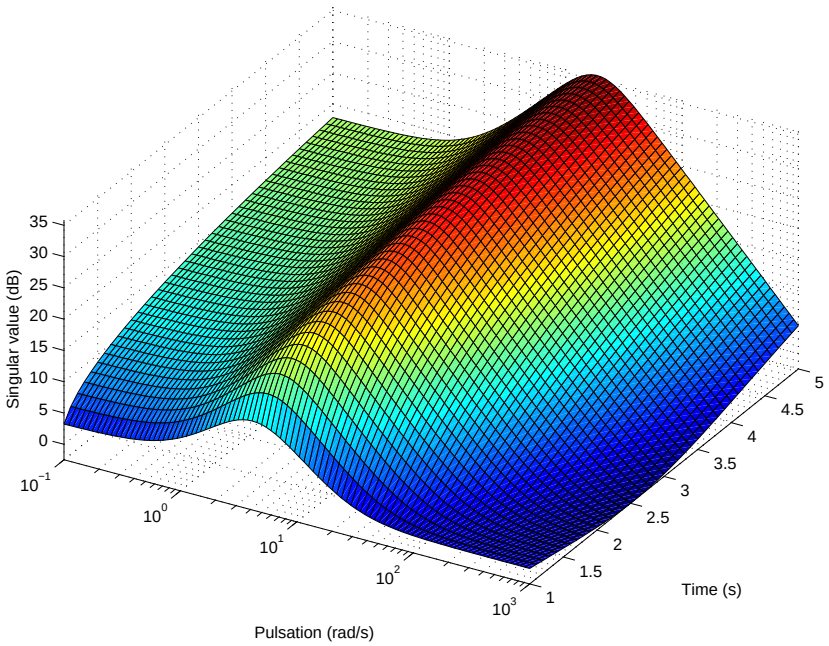

Figure 1.7: $K_{observer-based}(s,t)$: singular value w.r.t time.

1.4 Cross standard form

In most practical applications, the control design problem can be expressed in the following terms: is it possible to improve a given controller (often, a simple low-order controller designed upon a particular know-how or good sense rules) to meet additional H_2 or H_∞ specifications? or in other terms: is it possible to take into account a given controller (which meets some closed-loop specifications) in a standard H_2 and H_∞ control problem? To address this problem, the notion of Cross Standard Form (CSF) is introduced in this section for a given nth-order plant and an arbitrary given stabilizing n_Kth-order controller. The CSF can be seen as a solution for both inverse H_∞ and H_2 optimal control problems, that is: the CSF is a standard augmented problem whose **unique** H_∞ and H_2 optimal controller is an arbitrary given controller. The CSF is directly defined by the 4 state space matrices of the plant, the 4 state space matrices of the given controller and the solution T to the general non-symmetric Riccati equation (1.16) introduced in section 1.2 to compute the observer-based realization of a given controller for a given plant. The CSF can be applied to full-order, low-order or augmented-order controllers.

The interest for inverse optimal control problems motivates lots of works ([19], [24], [13],[17],[14] [27]). The practical interest of such solutions lies in the possibility to mix various approaches or take into account different kind of specifications ([31], [30], [28]). In the particular case of the H_∞ optimal control problem, the various contributions address restrictive cases: state feedback controller in [14], single-output single-output controller and specific sensitivity problem in [17]. But a solution for the general case (multi input multi-output, dynamic output feedback of arbitrary order) has never been stated. This general case is addressed in [27]: for a given weight system $W(s)$ and a given controller $K(s)$, the problem is to find all the plants $G(s)$ such that $\|F_l(F_l(W,G),K)\|_\infty < \gamma$ (see Figure 1.8). Note that the problem considered in this section is different since the plant $G(s)$ (that is, the lower right-hand transfer matrix of the standard augmented plant $P = F_l(W,G)$) is given and corresponds to the model of the plant between the control input and the measured output.

The convex closed-loop technique [9] seems also an attractive approach to take into account a given controller and additional H_2 or H_∞ constraints. But such an approach needs a Youla parameterization of the controller and so is limited to full-order (observer-based) controllers. Furthermore, this approach leads to very high order controller.

In section 1.4.1, the CSF is defined as a solution to H_2 and H_∞ inverse optimal control problems, for an nth-order Linear Time Invariant (LTI) system and a n_Kth-order stabilizing LTI controller. In section 1.4.2, an analytical expression of a CSF

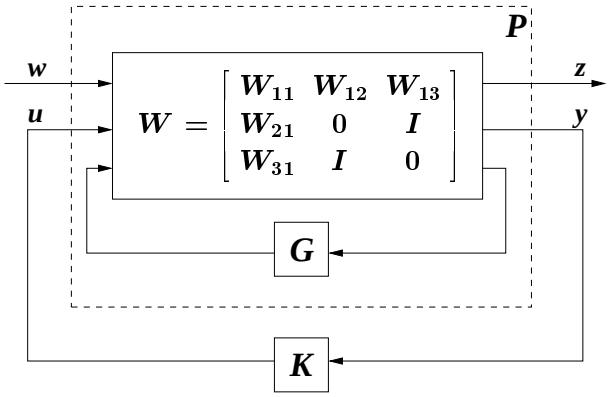

Figure 1.8: Block diagram of standard plant P, weight function W, model G and controller K.

is proposed for low-order controllers ($n_K \leq n$) and the existence of such a CSF is discussed. In section 1.12, this new CSF is extended for augmented-order controllers and so encompasses previous results presented in [5]. Finally, the missile second order example is used in section 1.4.4 to highlight the way to use CSF to take into account an initial low-order compensator and a frequency-domain specification in an augmented standard problem.

1.4.1 Definitions

The general standard plant between exogenous input w, control input u, controlled output z and measurement output y is denoted:

$$P(s) = \begin{bmatrix} P_{zw}(s) & P_{zu}(s) \\ P_{yw}(s) & P_{yu}(s) \end{bmatrix},$$

with corresponding state space realization:

$$P(s) := \left[\begin{array}{c|cc} A_p & B_1 & B_2 \\ \hline C_1 & D_{11} & D_{12} \\ C_2 & D_{21} & D_{22} \end{array}\right]. \tag{1.70}$$

Let us consider again the plant $G(s)$ defined in (1.2) and the stabilizing initial controller $K_0(s)$ defined by (1.5).

Definition 1 (Inverse H_2 optimal problem)
Find a standard plant $P(s)$ such that:

- $P_{yu}(s) = G(s)$,
- K_0 *stabilizes* $P(s)$,
- $K_0(s) = \arg\min_{K(s)} \|F_l(P(s), K(s))\|_2$,

(namely: $K_0(s)$ *minimizes* $\|F_l(P(s), K(s))\|_2$*).*

Definition 2 (Inverse H_∞ optimal problem)
Find a standard plant $P(s)$ *such that:*

- $P_{yu}(s) = G(s)$,
- K_0 *stabilizes* $P(s)$,
- $K_0(s) = \arg\min_{K(s)} \|F_l(P(s), K(s))\|_\infty$.

Definition 3 (Cross Standard Form)
If the standard plant $P(s)$ *is such that the 4 conditions:*

- ***C1****:* $P_{yu}(s) = G(s)$,
- ***C2****:* K_0 *stabilizes* $P(s)$,
- ***C3****:* $F_l(P(s), K_0(s)) = 0$,
- ***C4****:* K_0 *is the unique solution of the optimal* H_2 *or* H_∞ *problem* $P(s)$,

are met, then $P(s)$ *is called the Cross Standard Form (CSF) associated with the system* $G(s)$ *and the controller* $K_0(s)$ *and will be denoted* $P_{CSF}(s)$ *in the sequel.*

By construction, the CSF solves the inverse H_2 optimal problem and the inverse H_∞ optimal problem. Note that the uniqueness condition **C4** is relevant in our context since we are looking for an H_2 or H_∞ design to recopy a given controller.

1.4.2 Low-order controller case ($n_K \leq n$)

The following proposition provides a general analytical characterization of the CSF.

Proposition 1.4.1 *For a given stabilizable and detectable nth order system $G(s)$ (equation (1.2)) and a given stabilizing n_Kth order controller $K_0(s)$ with $n_K < n$ (equation (1.5)), a CSF reads:*

$$\boxed{P_{CSF}(s) := \left[\begin{array}{c|cc} A & T^{\#}B_K - BD_K & B \\ \hline -C_K T - D_K C & D_K D D_K - D_K & I_m - D_K D \\ C & I_p - D D_K & D \end{array}\right]} \tag{1.71}$$

where T is the solution of the generalized Riccati *equation (1.16) and where $T^{\#}$ is a right inverse* [5] *of T (such that $TT^{\#} = I_{n_K}$).*

Proof: from (1.71), it is obvious that conditions **C1** and **C2** are met. A state space realization of $F_l(P_{CSF}, K_0)$ associated with state vector $[x^T, \quad x_K^T]^T$ reads:

$$\left[\begin{array}{cc|c} A + BJ_m D_K C & BJ_m C_K & T^{\#}B_K \\ B_K J_p C & A_K + B_K D J_m C_K & B_K \\ \hline -C_K T & C_K & 0 \end{array}\right]$$

where J_m and J_p are defined in (1.6). Let us consider the change of state coordinates (already defined in equation (1.14)) :

$$\mathcal{M} = \mathcal{M}^{-1} = \left[\begin{array}{cc} I_n & 0 \\ T & -I_{n_K} \end{array}\right] \tag{1.72}$$

where T is a solution of (1.16) and $TT^{\#} = I_{n_K}$. The new state space realization of $F_l(P_{CSF}, K_0)$ reads:

$$\left[\begin{array}{cc|c} A + BJ_m(D_K C + C_K T) & -BJ_m C_K & T^{\#}B_K \\ 0 & A_K + (B_K D - TB)J_m C_K & 0 \\ \hline 0 & -C_K & 0 \end{array}\right] \tag{1.73}$$

So the $n + n_K$ stable close-loop eigenvalues are composed of:

- n eigenvalues of $A + BJ_m(D_K C + C_K T)$ which are unobservable by the controlled output z of P_{CSF},

[5] see also proposition 1.4.2.

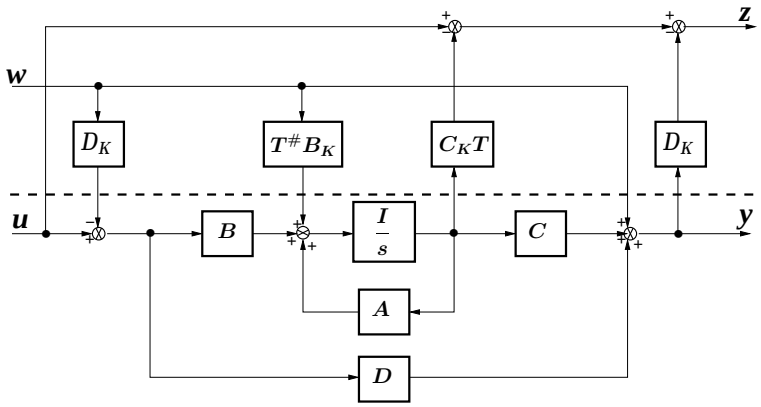

Figure 1.9: Block-diagram of Cross Standard Form $P_{CSF}(s)$ (case $n_K \leq n$).

- n_K eigenvalues of $A_K + (B_K D - TB)J_m C_K$ which are uncontrollable by the exogenous input w of P_{CSF}.

Thus, condition **C3** is met:

$$F_l(P_{CSF}(s), K_0(s)) = 0 \ .$$

In the next section it is shown that it is always possible de find a right inverse $T^{\#}$ of T such that the uniqueness condition **C4** is met and that ends the proof.

□

The general block-diagram associated with P_{CSF} is depicted in Figure 1.9. One can notice that the CSF is a one block problem and can be seen as a combination of well-known Output Estimation (OE) problem and Disturbance Feed-forward (DF) problem [36]. So, if both cross transfers ($P_{zu}(s)$ and $P_{yw}(s)$) are minimum phase (no zero in the closed right half plane), then both H_2 and H_∞ syntheses converge towards the same H_∞ performance index (γ) [35]. But for the standard problem P_{CSF}, one can state that $\gamma = 0$ and that both syntheses are exactly equal.

Uniqueness condition

The uniqueness condition (**C4**) can be proven considering the H_2-optimal controller of P_{CSF}: first of all, to vanish the direct feed-trough between exogenous inputs and controlled outputs in P_{CSF}, a simple change of variable ($u \leftarrow u - D_K y$) is performed

to transform P_{CSF} into the problem $\overline{P_{CSF}}(s)$:

$$\left[\begin{array}{c|cc} A+BJ_mD_KC & T^{\#}B_K & BJ_m \\ \hline -C_KT & 0 & I_m \\ J_pC & I_p & DJ_m \end{array}\right] \tag{1.74}$$

and thus:

$$\begin{aligned} F_l(P_{CSF},K) &= F_l(\overline{P_{CSF}},K-D_K)\,, \\ \arg\min_K \|F_l(P_{CSF},K)\| &= \arg\min_K \|F_l(\overline{P_{CSF}},K)\| + D_K\,. \end{aligned}$$

In [12, 36], it is demonstrated that a standard problem P has a unique H_2-optimal controller if and only if P is a regular problem. That is, in our case, if cross transfers $P_{zu}(s) := \left[\begin{array}{c|c} A+BJ_mD_KC & BJ_m \\ \hline -C_KT & I_m \end{array}\right]$ and $P_{yw}(s) := \left[\begin{array}{c|c} A+BJ_mD_KC & T^{\#}B_K \\ \hline J_pC & I_p \end{array}\right]$ have no invariant zeros on the $j\omega$ axis. It is clear that the n zeros of $P_{zu}(s)$ are the n eigenvalues of $\phi_{zu} = A + BJ_m(D_KC + C_KT)$ (ϕ_{zu} is the dynamic matrix of $P_{zu}^{-1}(s)$) and, considering (1.73), belong to the set of $n+n_K$ closed-loop eigenvalues and thus, are stable by assumption. **So, $P_{zu}(s)$ has no zeros on the $j\omega$ axis.**

The problem of the zeros of $P_{yw}(s)$ is more complex: the n zeros of $P_{yw}(s)$ are the n eigenvalues of $\phi_{yw} = A + BJ_mD_KC - T^{\#}B_KJ_pC$ (ϕ_{yw} is the dynamic matrix of $P_{yw}^{-1}(s)$). Then, pre-multiplying ϕ_{yw} by $N = [T^{\#} \quad T^{\perp}]$, post-multiplying by $N^{-1} = [T^T \quad T^{\perp}]^T$ and using (1.16) it comes:

$$N^{-1}\phi_{yw}N = \left[\begin{array}{cc} A_K + (B_KD - TB)J_mC_K & 0 \\ \star & T^{\perp T}(A + BJ_mD_KC - T^{\#}B_KJ_pC)T^{\perp} \end{array}\right].$$

The n zeros of $P_{yw}(s)$ are therefore composed of:

- n_K eigenvalues of $A_K + (B_KD - TB)J_mC_K$. Considering (1.73), these eigenvalues belong to the set of $n+n_K$ closed-loop eigenvalues and thus, are stable by assumption,
- $n - n_K$ eigenvalues of $\varphi(T^{\#}) = T^{\perp T}(A + BJ_mD_KC - T^{\#}B_KJ_pC)T^{\perp}$ whose location in the complex plane is discussed in the following proposition.

Proposition 1.4.2 *It is always possible to find a right inverse $T^{\#}$ of T such that all the $n - n_K$ eigenvalues of $\varphi(T^{\#})$ (and thus all the n zeros of the cross transfer P_{yw}) are not on the $j\omega$ axis.*

Proof: the set of right-inverse matrices of T can be parameterized in the following way:

$$T^{\#} = T^{+} + T^{\perp}X$$

where X is a $(n - n_K) \times n_K$ matrix of free parameters. Then:

$$\varphi(T^{\#}) = \varphi(X) = {T^{\perp}}^{T}(A + BJ_mD_KC)T^{\perp} - XB_KJ_pCT^{\perp} \; . \tag{1.75}$$

So, X allows the $n - n_K$ eigenvalues of φ to be assigned in the s-plane. The computation of X is in fact an eigenvalue assignment problem by a state feedback X^T on the pair $({T^{\perp}}^{T}(A + BJ_mD_KC)^{T}T^{\perp}, (B_KJ_pCT^{\perp})^{T})$.

□

So, the proposition 1.4.2 allows to state that $P_{zu}(s)$ **has no zeros on the** $j\omega$ **axis**. Thus $\overline{P_{CSF}}(s)$ is regular and $K_0(s)$ is the unique solution of the H_2-optimal problem P_{CSF}.

As $F_l(P_{CSF}, K_0) = 0$, all controllers solution of the H_∞-optimal problem are also solutions of the H_2-optimal problem. Thus $K_0(s)$ is also the unique solution of the H_∞-optimal problem P_{CSF}.

Existence of a CSF

Proposition 1.4.3 *The non-existence of a full row rank matrix T solution of the generalized non-symmetric* Riccati *equation (1.16) implies the non-existence of a CSF for $G(s)$ and $K_0(s)$.*

Contrariwise prof: let us assume that a regular CSF exists for the strictly proper stabilizing controller $K_0(s) - D_K$ and for the stabilizable and detectable modified system $\overline{G}(s)$ (such a change of variable is not restrictive):

$$\overline{G}(s) := \left[\begin{array}{c|c} A + BJ_mD_KC & BJ_m \\ \hline J_pC & DJ_m \end{array}\right] \; .$$

Then it is shown in [12] that the unique solution $\widehat{K_{H_2}}$ of the corresponding H_2-optimal problem involves a state feedback gain K_c and a state estimator gain K_f (according to the structure depicted in Figure 1.3 with $Q(s) = 0$). The n-th order state space realization of such a controller associated with the state vector $\widehat{x}$ reads:

$$\widehat{K_{H_2}} := \left[\begin{array}{c|c} A + BJ_mD_KC - BJ_mK_c - K_fJ_pC + K_fDJ_mK_c & K_f \\ \hline -K_c & 0 \end{array}\right] \; . \tag{1.76}$$

As the solution is unique: $\widehat{K_{H_2}}(s) = K_0(s) - D_K$. Thus the state space realization (1.76) is non-minimal if $n_K < n$. Thus a projection matrix $S_{n_K \times n}$ (full-row rank) exits such that: $x_K = S\widehat{x}$ and

$$\begin{aligned} S(A + BJ_mD_KC - BJ_mK_c - K_fJ_pC + K_fDJ_mK_c) &= A_KS \\ SK_f &= B_K \\ -K_c &= C_KS \ . \end{aligned}$$

Thus S solves the following equation:

$$S(A + BJ_mD_KC) + SBJ_mC_KS - B_KJ_pC - (A_K + B_KDJ_mC_K)S = 0 \ . \qquad (1.77)$$

This equation is exactly the same as the RICCATI equation (1.16) in T. Thus, **If T (or S) does not exist, then the Cross Standard Form for given $\overline{G}(s)$ and $K_0(s) - D_K$ (or $G(s)$ and $K_0(s)$) does not exist.**

□

Remark 1.4.4 *This last proposition highlights that the controller $\widehat{K}(s)$ provided by H_2 or H_∞ design on P_{CSF} is non-minimal. It can be shown that the $n - n_K$ non-minimal dynamics in $\widehat{K}(s)$ are assigned to the eigenvalues of $\varphi(X)$ (equation (1.75)) and thus can be assigned by a suitable choice of X (see example in section 1.4.4).*

1.4.3 Augmented-order controller case ($n_K > n$)

In the case $n_K > n$, the Cross Standard Form is directly defined from the 3 parameters K_c, K_f and $Q(s)$ of the observer-based realization of $K_0(s)$ (see Figure 1.10 and see [5] for the proof). These parameters can be computed using the procedure presented in section 1.2.3.

1.4.4 Illustration

The results of this section are illustrated on the missile example $G(s)$ presented in section 1.3. Let us consider the system described in equation (1.67) and the initial controller

$$K_0(s) = \frac{-23s - 32}{s + 12} = -23\frac{s + 1.391}{s + 12} := \left[\begin{array}{c|c} -12 & 4 \\ \hline 61 & -23 \end{array}\right] \ .$$

The only real solution T of (1.16) reads :

$$T = [0.32787 \quad -0.032787] \ .$$

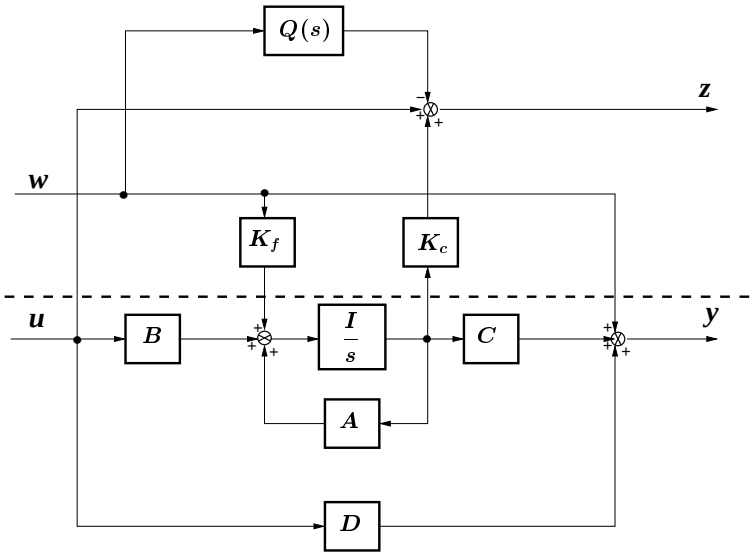

Figure 1.10: Block diagram of *Cross Standard Form* P_{CSF} (case $n_K > n$).

Let us choose $T^{\#} = T^{+}$, then the CSF (equation (1.71)) reads:

$$P_{CSF} := \left[\begin{array}{cc|cc} 0 & 1 & 12.079 & 0 \\ 1 & 0 & 21.792 & 1 \\ \hline 3 & 26 & 23 & 1 \\ 1 & 0 & 1 & 0 \end{array}\right] .$$

It is easy to check that the optimal H_∞ controller reads:

$$K_\infty(s) = -23\frac{(s+1.391)(s+2.079)}{(s+12)(s+2.079)}.$$

The corresponding MATLAB sequence using function `cor2tfg` [6] is:

```
a=[0 1;1 0];b=[0;1];c=[1 0];d=0;
AK=-12;BK=4;CK=61;DK=-23;
T=cor2tfg(pck(a,b,c,d),pck(AK,BK,CK,DK))
Tm1=pinv(T);
plant=pck(a,[Tm1*BK-b*DK b],[-CK*T-DK*c;c],...
     [-DK+DK*d*DK,eye(size(d,2))-DK*d;eye(size(d,1))-d*DK d]);
K=hinfsyn(plant,1,1,0,1000,0.01);
[ak,bk,ck,dk]=unpck(K);
zpk(ss(ak,bk,ck,dk))
```

[6] See :`http://personnel.supaero.fr/alazard-daniel/demos/demo_obr.html` .

Furthermore, equation (1.75) reads:

$$\varphi(X) = -2.0792 - 0.39801\,X \quad \text{and} \quad \varphi(246.02294) = -100\ .$$

Then the choice:

$$T^{\#} = T^{+} + 246.0229T^{\perp} = [27.5 \quad 244.5]^{T}$$

leads to a new P_{CSF} and a new optimal H_∞ controller:

$$K_\infty(s) = -23\frac{(s+1.391)(s+100)}{(s+12)(s+100)}.$$

In both designs, K_∞ is not minimal and $K_\infty = K_0$.

Improving K_0 with frequency domain specification

In fact, K_0 has been designed to assign the dominant closed-loop eigenvalues to $-1 \pm i$. Indeed:

$$\text{poles of } \frac{1}{1 - K_0(s)G(s)} = \{-1+i,\ -1-i,\ -10\}.$$

The magnitude of the frequency-domain response of $K_0(s)$ is plotted in Figure 1.11 (solid line). Now, let us assume we want the controller to have a roll-off behavior beyond $10\,rd/s$ and must fulfill the low-pass template also depicted in Figure 1.11 (grey patch). Such a specification can be formulated to attenuate missile flexible modes which are not taken into account in the design model $G(s)$.

This specification can be handled, in H_∞ framework, in weighting the closed-loop transfer from a disturbance on the plant output (measurement noise) to the plant input u [7]. It is obvious that, in the standard problem associated to the CSF (see Figure 1.9), the plant input u is directly linked to the controlled output z. Then, in order to take into this frequency-domain specification, one can augment this standard problem with a noise w' acting on the measurement y and weighted by a second order high pass filter (in order to get a $-40\,dB/dec$ roll-off behavior). The augmented CSF is then depicted in Figure 1.12. The high-pass filter $W(s)$ is in fact a second order derivative filter whose poles ($\frac{-1000}{\sqrt{2}}(-1 \pm i)$) are introduced for properness reasons. The gain g is tuned by a try and error procedure. The tuning $g = 0.02$ provides a 4th-order H_∞ optimal controller $K(s)$ whose frequency response is depicted in Figure 1.11 (dashed line). The template is now fulfilled and

[7] Such a transfer reads: $K(I_m - KG)^{-1}$ (with positive feedback).

one can check that the closed-loop dominant dynamics is assigned to the nominal values $-1 \pm i$. Indeed:

$$\text{poles of } \frac{1}{1 - K(s)G(s)} = \{-1 \pm i,\ -9.7947,\ -14.272 \pm 12.985\, i,\ -1424.5\}.$$

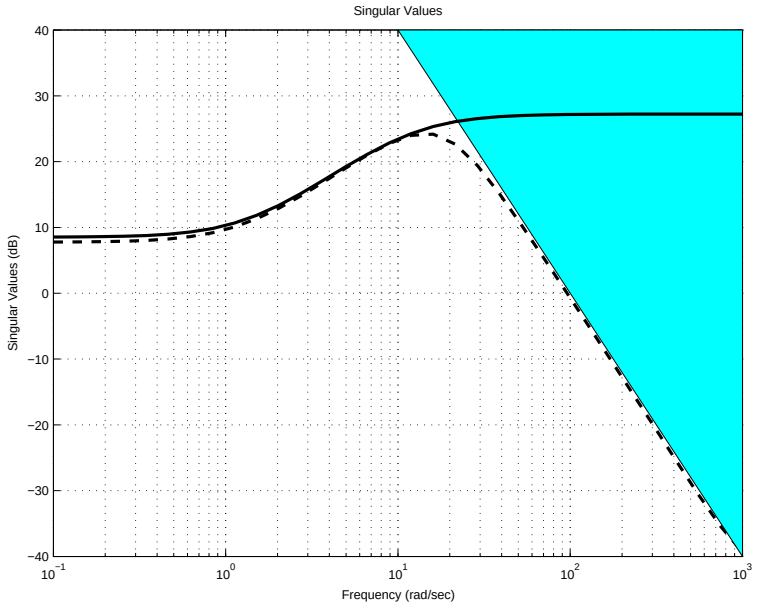

Figure 1.11: Frequency-domain responses (magnitude) of $K_0(s)$ (solid line) and $K(s)$ (dashed line) and template (grey patch).

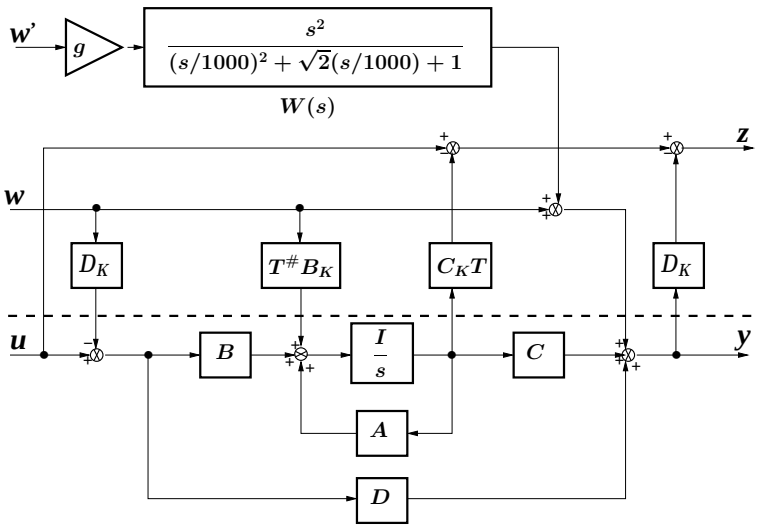

Figure 1.12: Augmented Cross Standard Form to take into account roll-off specification (with $T^{\#} = [27.5 \quad 244.5]^T$).

1.5 Discrete-time case

Techniques presented in sections 1.2 and 1.4 in the continuous-time case are now extended to the discrete-time case (proofs are omitted for brevity).

The discrete-time plant $G(z)$ (order n) is defined as :

$$\left\{ \begin{array}{lcl} x(k+1) & = & Ax(k) + Bu(k) \\ y(k) & = & Cx(k) + Du(k) \end{array} \right. \tag{1.78}$$

The discrete-time controller $K_0(z)$ (order n_K) is defined as :

$$\left\{ \begin{array}{lcl} x_K(k+1) & = & A_K x_K(k) + B_K y(k) \\ u(k) & = & C_K x_K(k) + D_K u(k) \end{array} \right. \tag{1.79}$$

Two classical implementation structures of discrete-time observer-based controllers can be used: the predictor and the estimator structures.

1.5.1 Discrete-time predictor form

The predictor form is described by :

$$\left\{\begin{array}{lcll} \widehat{x}(k/k) & = & A\widehat{x}(k/k-1)+Bu(k) & \text{Prediction} \\ \widehat{x}(k+1/k) & = & \widehat{x}(k/k)+K_f(y(k)-C\widehat{x}(k/k-1)-Du(k)) & \text{Correction} \\ u(k+1) & = & -K_c\widehat{x}(k+1/k) & \text{Control} \end{array}\right. \tag{1.80}$$

This case is analogous to the continuous-time one. The construction procedure is therefore the same. It provides the parameters K_c^p, K_f^p, A_Q^p, B_Q^p, C_Q^p and D_Q^p of the Youla-parameterization associated with the predictor form whose state-space representation reads :

$$\left\{\begin{array}{lcl} \widehat{x}(k+1/k) & = & A\widehat{x}(k/k-1)+Bu(k)+K_f^p(y(k)-C\widehat{x}(k/k-1)-Du(k)) \\ x_Q(k+1) & = & A_Q^p x_Q(k)+B_Q^p(y(k)-C\widehat{x}(k/k-1)-Du(k)) \\ u(k) & = & -K_c^p\widehat{x}(k/k-1)+C_Q^p x_Q(k)+D_Q^p(y(k)-C\widehat{x}(k/k-1)-Du(k)) \end{array}\right. \tag{1.81}$$

1.5.2 Discrete-time estimator-form

The estimator structure of an observer-based controller is now described as :

$$\left\{\begin{array}{lcll} \widehat{x}(k+1/k) & = & A\widehat{x}(k/k)+Bu(k) & \text{Prediction} \\ \widehat{x}(k+1/k+1) & = & \widehat{x}(k+1/k)+K_f(y(k+1)-C\widehat{x}(k+1/k)-Du(k+1)) & \text{Correction} \\ u(k+1) & = & -K_c\widehat{x}(k+1/k+1) & \text{Control} \end{array}\right. \tag{1.82}$$

In contrast to the previous case, this discrete-time estimator controller exhibits a direct feed-through between $y(k)$ and $u(k)$ but the separation principle still holds : the closed-loop transfer function between the input reference and the innovation $y(k)-C\widehat{x}(k/k-1)-Du(k)$ is zero and the closed-loop poles can be splitted into the closed-loop state-feedback poles ($\text{spec}(A-BK_c)$) which are unobservable from the innovation, and the closed-loop state-estimator poles ($\text{spec}(A(I-K_fC))$) which are uncontrollable by the reference input. The Youla-parameterization associated with this structure is depicted in Figure 1.13 and reads :

$$\left\{\begin{array}{lcl} \widehat{x}(k+1/k) & = & A\widehat{x}(k/k-1)+Bu(k)+AK_f(y(k)-C\widehat{x}(k/k-1)-Du(k)) \\ x_Q(k+1) & = & A_Q x_Q(k)+B_Q(y(k)-C\widehat{x}(k/k-1)-Du(k)) \\ u(k) & = & -K_c\widehat{x}(k/k-1)+C_Q x_Q(k)+(D_Q-K_cK_f)(y(k)-C\widehat{x}(k/k-1)-Du(k)) \end{array}\right. \tag{1.83}$$

We know from sections 1.2 and 1.5.1 how to compute all the parameters (K_c^p, K_f^p, A_Q^p, B_Q^p, C_Q^p and D_Q^p) of the predictor form and the corresponding Youla parameterization, from a given compensator ($A_K,\ B_K,\ C_K,\ D_K$) and a given plant

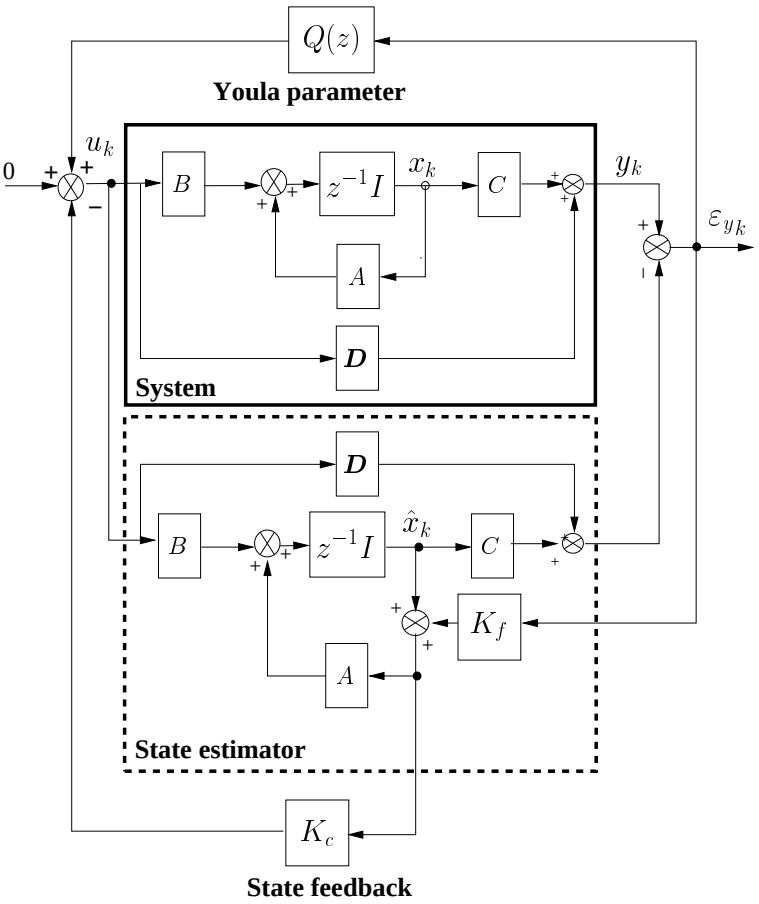

Figure 1.13: The discrete-time YOULA parameterization using state estimator structure (where $\widehat{x}_k = \widehat{x}(k/k-1)$).

$(A,\ B,\ C,\ D)$. As a consequence, the parameters (K_c, K_f, A_Q, B_Q, C_Q and D_Q) of the equivalent estimator form can be obtained by direct identification of the representations (1.81) and (1.83). This yields :

$$\begin{array}{c} K_c = K_c^p,\ \ K_f = A^{-1}K_f^p, \\ A'_Q = A_Q^p,\ \ B_Q = B_Q^p,\ \ C_Q = C_Q^p,\ \ D_Q = D_Q^p + K_c^p K_f^p \end{array} \tag{1.84}$$

1.5.3 Discrete-time Cross Standard Form

In the case of low-order controller ($n_K \leq n$), the general expression for the CSF (equation 1.71) is valid for the discrete-time case.

In the case of augmented-order controller ($n_K \geq n$), it is possible to define the CSF associated with an estimator form of the controller (1.83), This CSF reads :

$$P_{CSF}(z) := \left[\begin{array}{cc|cc} A & 0 & AK_f & B \\ 0 & A_Q & B_Q & 0 \\ \hline K_c & -C_Q & -D_Q + K_c K_f & I_m \\ C & 0 & I_p & D \end{array}\right]. \tag{1.85}$$

The block diagram associated with this Cross Standard Form is depicted in Figure 1.14.

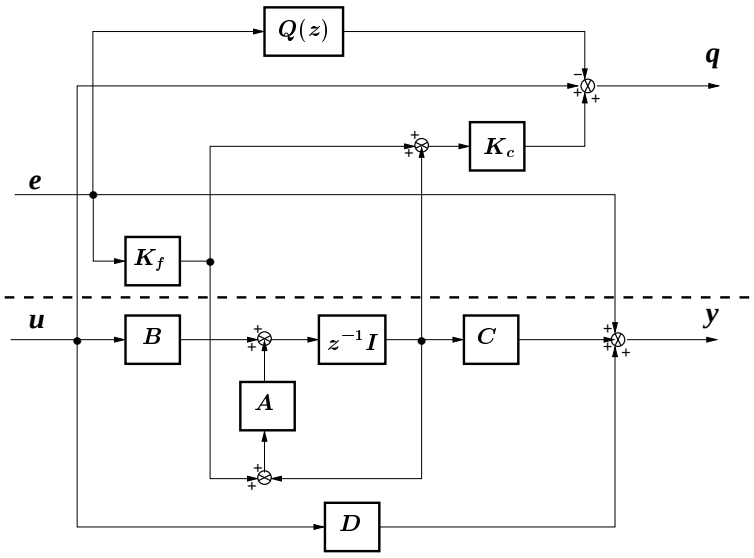

Figure 1.14: Discrete-time Cross Standard Form.

1.6 Launch vehicle control problem

CSF and gain scheduling using observer-based realization are illustrated in this section on a control design problem for a launch vehicle (representative of a strategic missile).

1.6.1 Description

This application considers the launch vehicle inner control loop. According to Figure

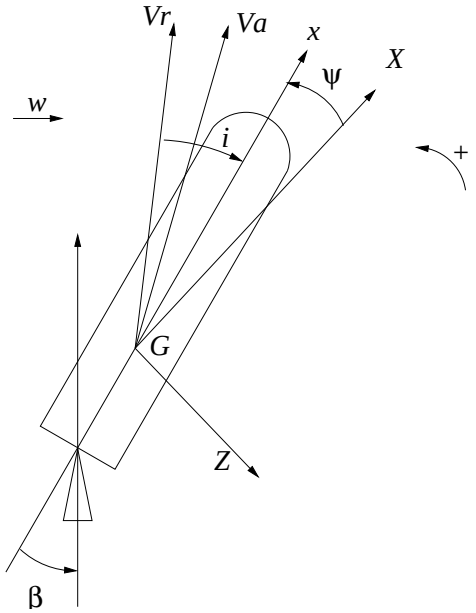

Figure 1.15: Launch vehicle simplified representation.

1.15, the following notation is used:

- i : the launch vehicle angle of attack,
- ψ : the deviation angle around axis w.r.t. the guidance attitude reference,
- V_a and V_r : respectively, the absolute and the relative velocity,
- w : the wind velocity,
- β : the thruster angle of deflection,

- $\dot{z}$: the lateral drift rate.

The rigid behavior is modelled by a third-order system with state vector :$x^r = [\ \psi \quad \dot{\psi} \quad \dot{z}\ ]^T$. This rigid model strongly depends on 2 uncertain dynamic parameters A_6 (aerodynamic efficiency) and K_1 (thruster efficiency).
From Figure 1.15 and under small angle assumption, one can derive the angle of attack equation :

$$i = \psi + \frac{\dot{z} - w}{V} \ . \tag{1.86}$$

The discrete-time validation model considered in this section (that is the full-order model $G_f(z)$) is characterized by the rigid dynamics, the dynamics of thrusters (order 2), sensors (order 2) and the first 5 bending modes (order 10). The launch vehicle is aerodynamically unstable. Finally, the characteristics of bending modes are uncertain (4 uncertain parameters per mode).

1.6.2 Objectives

The available measurements are the attitude angle (ψ) and rate ($\dot{\psi}$). The control signal is the thruster deflection angle β. Launch vehicle control objectives for the whole atmospheric flight phase are as follows:

- performance with respect to disturbances (wind): the angle of attack peak, in response to the typical wind profile $w(t)$, must stay within a narrow band ($\pm\ i_{max}$). This wind profile is plotted in Figure 1.16 (dashed plot) and corresponds to a worst case wind encountered during launches with a strong gust when aerodynamic pressure is maximal,

- closed-loop stability with sufficient stability margins. This involves constraints on the rigid mode but also on the flexible modes. In fact, the first flexible mode is "naturally" phase controlled (collocation between sensors and actuator) while other flexible modes must be gain controlled (roll-off). So, the peaks associated with the flexible modes (except for the first) on the frequency response of the loop gain ($L(s) = K(s)G(s)$) must stay below a specified level X_{dB} for all parametric configurations (see Figure 1.21 as an example). From the synthesis point of view, the flexible modes are not taken into account in the synthesis model. But a roll-off behavior with a cut-off frequency between the first and the second flexible modes must be specified in the synthesis,

- delay margin must be greater than one sampling period.

All these objectives must be achieved for all configurations in the uncertain parameter space (22 uncertain parameters including aerodynamics coefficient, propulsion efficiency and bending modes characteristics), particularly in some identified worst cases where the combination of parameter extremal values is particularly critical. In this paper, the robustness analysis is limited to these worst cases as the experience has shown that they are quite representative of the robustness problem. A more complete μ-analysis is presented in [16].

1.6.3 Launch vehicle control design

The approach proposed to satisfy all theses stationary objectives proceeds in 2 steps : the first one aims to satisfy time-domain specification (angle of attack constraint) and the second one is a H_∞ synthesis based on the CSF allowing the frequency-domain specifications (roll-off, stability margins) to be met.

The models used for the synthesis are discrete-time models including a zero-order hold.

First synthesis : non conventional LQG/LTR synthesis

State feedback on the rigid model

The standard control problem is characterized by 2 controlled outputs i and $\dot{z}$, 2 measurements ψ and $\dot{\psi}$, 1 control signal β and 1 exogenous input w (disturbance). This standard problem reads :

$$\left[\begin{array}{c} \dot{x^r} \\ \hline i \\ \hline \dot{z} \\ \hline \psi \\ \dot{\psi} \end{array}\right] = \left[\begin{array}{c|c|c} A & B_1 & B_2 \\ \hline C_1 & D_{11} & D_{12} \\ \hline C_2 & D_{21} & D_{22} \end{array}\right] \left[\begin{array}{c} x^r \\ \hline w \\ \hline \beta \end{array}\right] \tag{1.87}$$

Then, the gain K_d is computed such that the discrete-time control law $\beta_k = -K_d\, x_k^r$ minimizes the following continuous-time LQ criterium :

$$J = \int_0^\infty \left(\alpha \dot{z}^2 + i^2 + r\beta^2\right) dt = \int_0^\infty \left({x^r}^T Q x^r + \beta^T R \beta + 2 {x^r}^T N \beta \right) dt. \tag{1.88}$$

with:

$$Q = C_1^T \left[\begin{array}{cc} 1 & 0 \\ 0 & \alpha \end{array}\right] C_1, \quad R = r, \quad N = 0_{3\times 1}\ .$$

The model and the performance index are discretized by taking into account the zero-order hold at the input β_k:

$$J_d = \sum_{k=1}^{\infty} ({x_k^r}^T Q_d x_k^r + \beta_k^T R_d \beta_k + 2{x_k^r}^T N_d \beta_k) \tag{1.89}$$

for the discrete-time model $x_{k+1}^r = A_d x_k^r + B_{2_d}\beta_k$. The matrices ($A_d$, B_{2_d}, Q_d, N_d and R_d) involving the matrix exponential are computed using the Van Loan's Formula [22].
Adopting the notation :

$$K_d = [K_\psi,\, K_{\dot\psi},\, K_{\dot z}]\,, \tag{1.90}$$

the gain K_d can be used to built a servo-loop of the measured variable ψ, that is :

$$\beta_k = K_\psi(\psi_{ref_k} - \psi_k) - K_{\dot\psi}\dot\psi_k - K_{\dot z}\dot z_k \tag{1.91}$$

where ψ_{ref_k} is the input reference.

Augmented state with wind dynamic

The wind dynamics is modelled by a stable first-order filter and is then discretized with the zero-order hold method:

$$w_{k+1} = A_w w_k + \tilde w_k\ .$$

This disturbance feed-forward model introduces a new tuning parameter A_w. The discrete-time augmented problem corresponding to the state vector $x^a = [x^r,\ w]^T$ then reads :

$$\left[\begin{array}{c} x_{k+1}^a \\ \hline \dot\imath_k \\ \dot z_k \\ \hline \psi_k \\ \dot\psi_k \end{array}\right] = \left[\begin{array}{cc|c|c} A_d & B_{1_d} & 0 & B_{2_d} \\ 0 & A_w & I & 0 \\ \hline C_1 & D_{11} & 0 & D_{12} \\ \hline C_2 & D_{21} & 0 & D_{22} \end{array}\right] \left[\begin{array}{c} x_k^a \\ \hline \tilde w_k \\ \hline \beta_k \end{array}\right] = \left[\begin{array}{c|c|c} A_d^a & B_{1_d}^a & B_{2_d}^a \\ \hline C_1^a & 0 & D_{12} \\ \hline C_2^a & 0 & D_{22} \end{array}\right] \left[\begin{array}{c} x_k^a \\ \hline \tilde w_k \\ \hline \beta_k \end{array}\right] \tag{1.92}$$

with: $B_{1_d} = \int_0^{T_s} e^{A\eta} B_1\, d\eta$.

In order to compute the new state feedback gain K_d^a associated with the augmented state x^a, equation (1.91) is used with ψ_{ref_k} such that the angle of attack due to disturbance w is cancelled (see equation 1.86), that is :

$$\psi_{\mathrm{ref}_k} = \frac{w_k - \dot z_k}{V}.$$

Then, the term $\frac{\dot z_k}{V}$ is ignored because it can introduce non-stabilizing couplings in the lateral motion. Finally, the gain K_d^a is obtained as:

$$K_d^a = \left[\ K_d \quad -\tfrac{K_\psi}{V}\ \right]. \tag{1.93}$$

Following this procedure, the LQ state feedback closed-loop dynamics is stable and satisfies:

$$\text{spec}(A_d^a - B_{2_d}^a K_d^a) = \text{spec}(A_d - B_{2_d} K_d) \cup \text{spec}(A_w)$$

KALMAN*'s filter with LTR tuning*

To compute the gain G_d^a of the KALMAN's filter on the augmented model (A_d^a, $B_{2_d}^a$, C_2^a, D_{22}), an LTR tuning is proposed. It is well known that stability margins of the LQ state feedback are degraded when the KALMAN's filter is introduced in the control loop. The LTR procedure allows these stability margins to be recovered [6]. Thus, the state noise is composed of 2 disturbing signals: one on the wind model input ($\tilde{w}$) and one on the control input β through a gain $\sqrt{\rho}$ (LTR effect) :

$$W = \begin{bmatrix} \rho B_2 {B_2}^T & 0 \\ 0 & I \end{bmatrix} \quad \text{and} \quad V = v \begin{bmatrix} 1 & 0 \\ 0 & \omega_f^2 \end{bmatrix}$$

W and V are the covariance matrices of continuous-time noises on the state vector (x^a) and the measurement vector ($[\psi,\ \dot{\psi}]^T$), respectively. Therefore the KALMAN filter tuning depends on 3 parameters: ρ (LTR weighting), v (measurement to state noise ratio) and $\omega_f\,(rd/s)$ (rate to position measurement noise ratio). ω_f represents the frequency beyond which it is better to integrate the rate measurement $\dot{\psi}$ to estimate the position $\hat{\psi}$ than to use the measurement position ψ directly.

The covariance matrices, W_d and V_d, of discrete-time noises on the state vector and the measurement vector are also discretized using Van Loan's formulae.
This non conventional LQG/LTR design yields a 4th-order compensator $K_1(z)$ involving the gains K_d^a and G_a^d, the augmented model (A_d^a, $B_{2_d}^a$, C_2^a, D_{22}) and is defined by equation (1.83) without YOULA parameter $Q(z)$. The results obtained so far are presented in Figures 1.16 and 1.17.

In Figure 1.16 it can be observed that the performance requirements (angle of attack) are quite satisfied for all worst cases. In Figure 1.17, one can also note that the template for low frequency stability margins is satisfied (this templates is depicted in Figure 1.17 with the vertical line on the first critical point on the right-hand side) and the first flexible mode remains between two critical points for all worst cases (phase control). But the roll-off effect is not strong enough: the template for gain margins on flexible modes number 2 and 3 (depicted in Figure 1.17 with the horizontal line at $X\,dB$) is not satisfied in no case. Note that Nichols plots are obtained with discrete-time transfers: it appears that flexible modes 4 and 5 are aliasing between flexible modes 1 and 3. These modes are not significant for the control design.

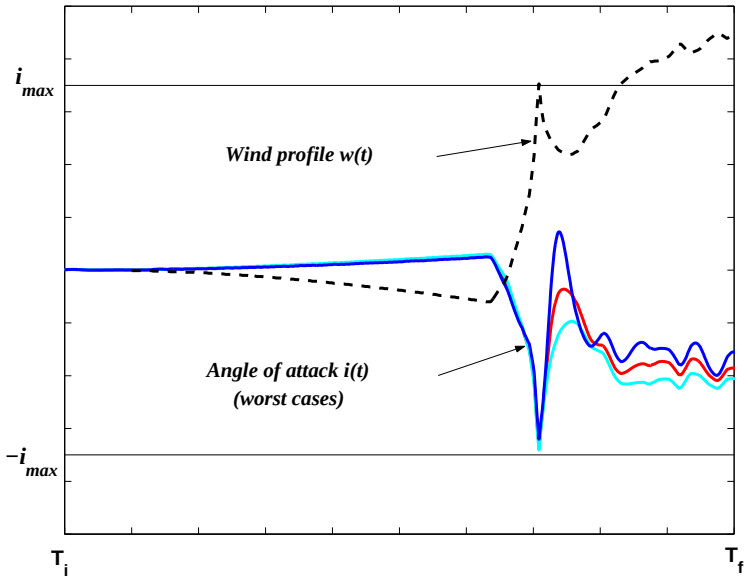

Figure 1.16: Angle of attack $i(t)$ (solid) obtained with $K_1(z)$ and wind profile $w(t)$ (dashed, normalized unit).

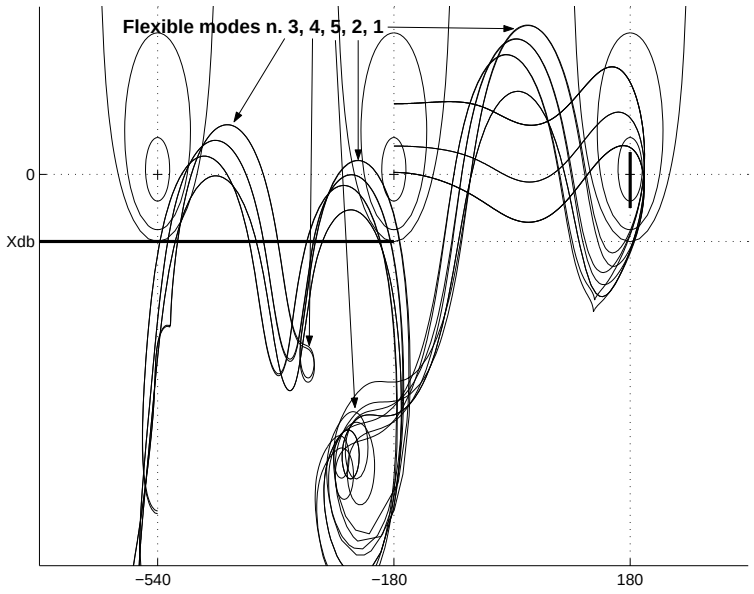

Figure 1.17: $K_1(z)G_f(z)$: NICHOLS's plots for worst cases.

Second synthesis : H_∞ synthesis using CSF for frequency-domain specifications

In order to satisfy this last frequency domain requirement, an H_∞ synthesis is performed on the standard problem depicted in Figure 1.18 :

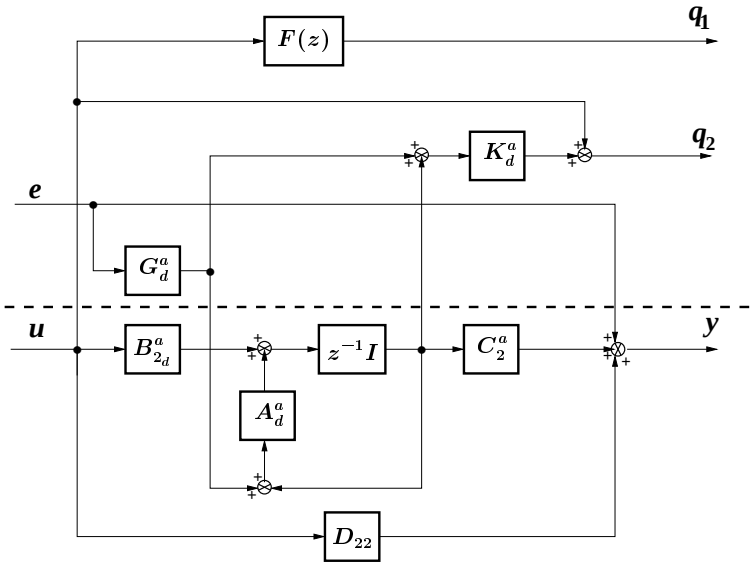

Figure 1.18: $P_f(z)$: setup for the final H_∞ synthesis.

This standard problem can be described as follows:

- between inputs $[e \quad u]^T$ and outputs $[q_2 \quad y]^T$, one can recognize the CSF presented in section 1.4 which will inflect the solution towards the previous pure performance compensator (LQG/LTR design),
- the output q_1 is introduced to specify the roll-off behavior with a 2nd-order filter $F(z)$ in order to fulfil the gain margin template on flexible modes number 2 and 3.

The output q_1 in fact weighs the 2nd-order derivative of the control signal u. The frequency domain response of $F(z)$ is depicted in Figure 1.19. This response exhibits a wide hump centered on the flexible modes 2 and 3. This hump frames peak variations of flexible modes 2 and 3 for all worst cases.

Then, the H_∞ synthesis provides a 6th-order compensator $K_2(z)$. Analysis results are displayed in Figures 1.20 and 1.21. The time-domain performance specifi-

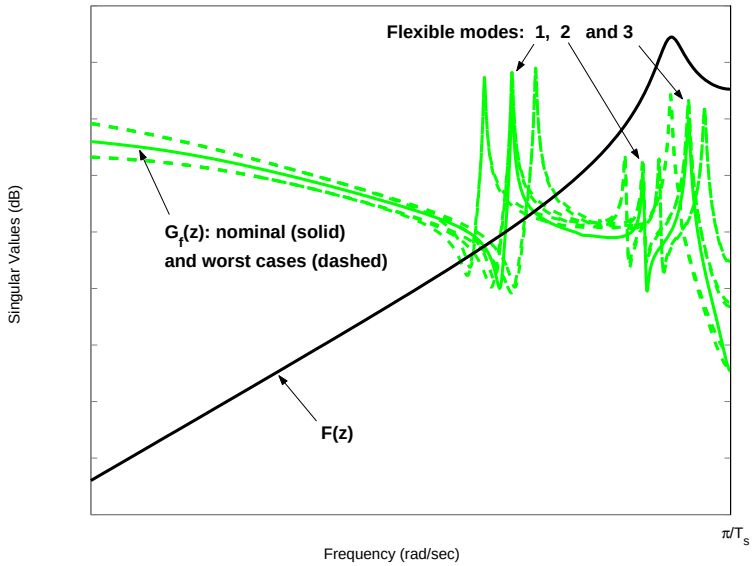

Figure 1.19: Singular values: $F(z)$ (black) and $G_f(z)$ (grey).

cation is still met (Figure 1.20). Figure 1.21 shows that stability margins are good enough for all worst cases and the roll-off behavior is now quite satisfactory.

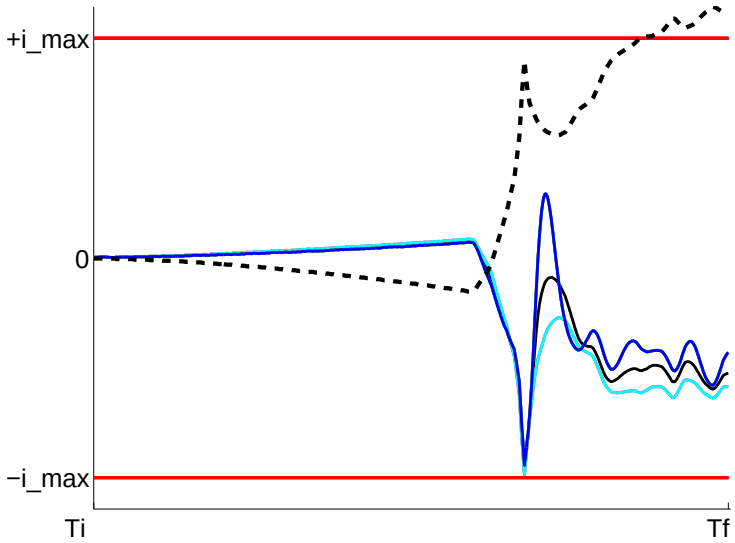

Figure 1.20: Angle of attack $i(t)$ (solid) obtained with $K_2(z)$ and wind profile $w(t)$ (dashed).

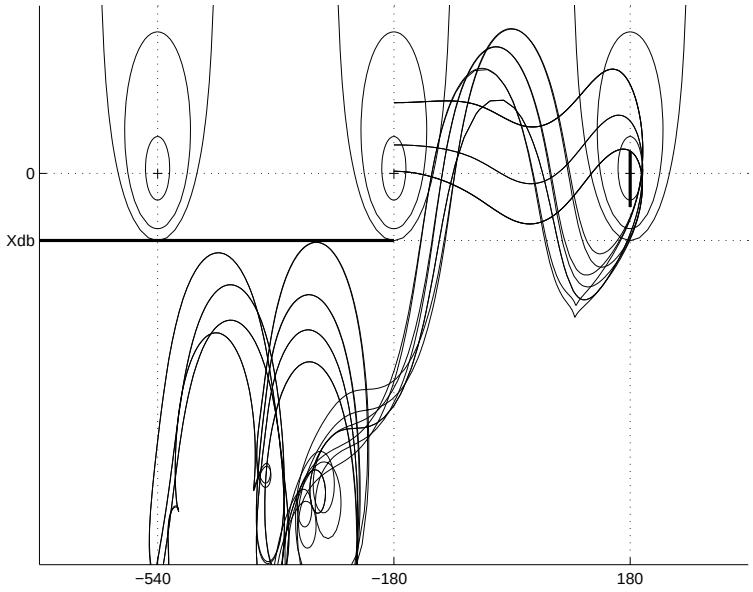

Figure 1.21: $K_2(z)G_f(z)$: NICHOLS's plots for worst cases.

1.6.4 Gain-scheduling

The previous stationary design has been applied for various instants t^i along the flight envelope. The H_∞ solver which has been used is the Matlab macro-function `dhinfric` because it provides the best index γ among the various algorithms proposed in the various Matlab toolboxes. The drawback of this algorithm lies in the fact that the solution $K_2^i(z)$ is not the central DGKF solution. Because of multiple variable changes performed to increase numerical conditioning in RICCATI equations, the realization of the solution has no physical meaning. The linear interpolation of the 4 matrices (A_K^i, B_K^i, C_K^i and D_K^i) provides a non-stationary compensator noted $K_2(z,t)$ with a awkward behavior as can be seen from the evolution of the singular value of $K_2(z,t)$ as a function of time t during the atmospheric flight (Figure 1.22).

This problem can be easily mastered using observer-based realizations. Thus, an observer-based realization of each compensator $K_2^i(z)$ is computed using the approach presented in 1.2. The model used in this realization is the transfer between u and y of the standard problem $P_f(z)$ (see Figure 1.18). The main difficulty with this approach is that the observer-based realization is not unique and depends on the way the closed-loop dynamics $F_l(P_f^i(z), K_2^i(z))$ is split between the state feedback dynamics and the state estimation dynamics. Considering the particular structure of the standard problem $P_f(z)$, this difficulty is easily overcame:

Let $\left[\begin{array}{c|c} A_F & B_F \\ \hline C_F & D_F \end{array}\right]$ be a realization of the weighting filter $F(z)$, then the realization of the augmented plant $P_f(z)$ depicted in Figure 1.18 is given as:

$$P_f(z) := \left[\begin{array}{ccc|c} A_d^a & 0 & A_d^a G_d^a & B_{2_d}^a \\ 0 & A_F & 0 & B_F \\ \hline 0 & C_F & 0 & D_F \\ \hline K_d^a & 0 & K_d^a G_d^a & 1 \\ \hline C_2^a & 0 & I_{2\times 2} & D_{22} \end{array}\right] = \left[\begin{array}{c|c|c} \mathcal{A} & \mathcal{B}_1 & \mathcal{B}_2 \\ \hline \mathcal{C}_1 & \mathcal{D}_{11} & \mathcal{D}_{12} \\ \hline \mathcal{C}_2 & I_{2\times 2} & D_{22} \end{array}\right] .$$

One can also derive:

$$\mathrm{spec}(\mathcal{A} - \mathcal{B}_1\mathcal{C}_2) = \mathrm{spec}(A_d^a(I - G_d^a C_2^a)) \cup \mathrm{spec}(A_F) .$$

The first term ($\mathrm{spec}(A_d^a(I - G_d^a C_2^a))$) represents the stable dynamics of the KALMAN filter previously designed. The second term ($\mathrm{spec}(A_F)$) stands for the roll-off filter dynamics which must be chosen stable. It can be shown that our standard problem $P_f(z)$ is a pure Disturbance Feed-forward (DF) problem (see [18] and appendix in [34]) and that half of the closed-loop dynamics of $F_l(P_f(z), K_2(z))$ will be assigned to $\mathrm{spec}(\mathcal{A}-\mathcal{B}_1\mathcal{C}_2)$ for any value of the final index γ. This dynamics must be assigned to the state estimation dynamics when one wants to find the equivalent observer-based of the compensator $K_2(z)$ using the procedure proposed in section 1.2. Then, the observer-based realization becomes unique.

Let us note $\left[\begin{array}{c|c} A_{LQG}^i & B_{LQG}^i \\ \hline C_{LQG}^i & D_{LQG}^i \end{array}\right] = \left[\begin{array}{c|c} \mathcal{A}^i - \mathcal{B}_2^i\mathcal{K}_c^i - \mathcal{K}_f^i\mathcal{C}_2^i + \mathcal{K}_f^i\mathcal{D}_{22}^i\mathcal{K}_c^i & \mathcal{K}_f^i \\ \hline \mathcal{K}_c^i & \mathcal{D}_Q \end{array}\right]$ the observer-based realization of each compensator $K_2^i(z)$. The linear interpolation of the 4 new matrices (A_{LQG}^i, B_{LQG}^i, C_{LQG}^i and D_{LQG}^i) provides a new non-stationary compensator noted $K_{LQG}(z,t)$. The evolution of the singular value of $K_{LQG}(z,t)$ w.r.t. time t is presented in Figure 1.23. This response is significantly smother than the one of Figure 1.22.

Figure 1.24 depicts the evolution of the stability margins during the whole atmospheric flight for all worst cases. Obtained margin to desired margin ratios (in percent) are plotted w.r.t time for the low frequency gain margin (LF margin: above the right-hand critical point in the NICHOLS chart), the high frequency gain margin (HF margin: under the right-hand critical point in the NICHOLS chart), the attenuation of the flexible modes below X_{dB} (corresponding to horizontal line in the NICHOLS chart) and the delay margin. One can notice that the specifications are met at each instant of the flight (ratios must be positive to fulfil specifications).

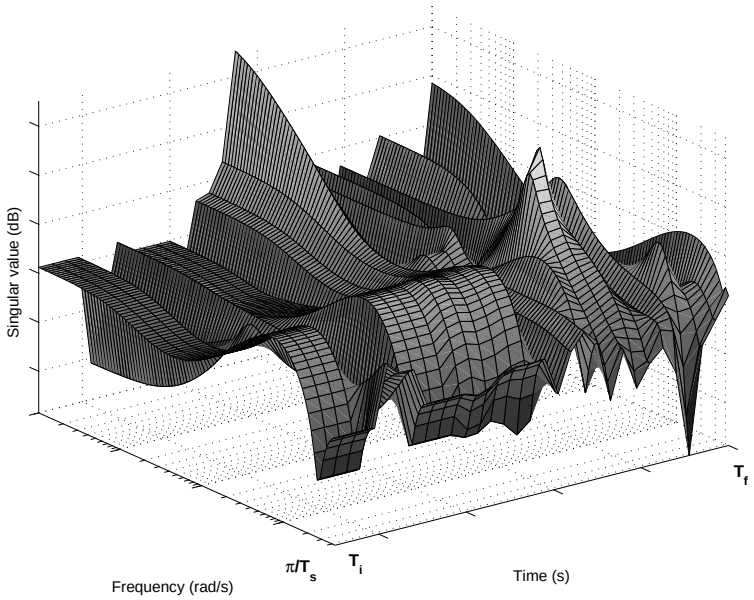

Figure 1.22: $K_2(z,t)$: singular value w.r.t time.

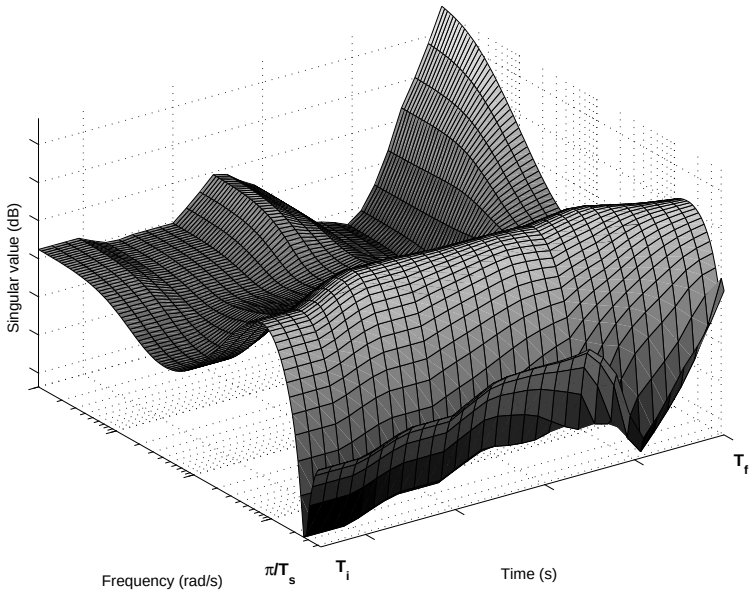

Figure 1.23: $K_{LQG}(z,t)$: singular value w.r.t time.

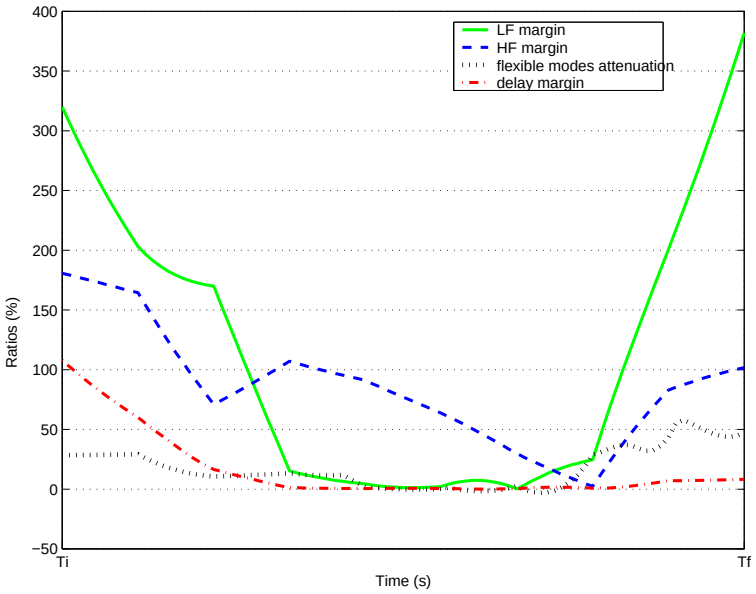

Figure 1.24: Obtained margin to desired margin ratios w.r.t. time.

1.7 Conclusions

In this chapter, a procedure to compute observer-based structures for arbitrary controllers was proposed. This technique is based upon the resolution of a generalized non-symmetric RICCATI equation. Necessary conditions were given for the solvability of this equation in terms of observability and controllability properties of the plant. The interest of observer-based realization for gain scheduling, controller switching and state monitoring was highlighted on a very simple example. Demo files are available for readers who wish to practice.

Further work is still needed to exploit the multiplicity of choices in the distribution of the closed-loop poles between the closed-loop state-feedback poles, the closed-loop state-estimator poles and the Youla parameter poles. This problem is particularly important to smoothly interpolate or schedule a family of state-feedback gains and state-estimator gains for practical problems requiring some gain-scheduling strategy. The usefulness of these controller structures to handle input saturation constraints is also deserves investigation.

The CSF was presented here as a particular solution of the inverse optimal control problem. The CSF can be used to mix various synthesis techniques in order to satisfy a multi-objective problem. Indeed, the general idea is to design a first controller to meet some specifications, mainly performance specification. Then, the

CSF is applied on this first solution to initialize a standard problem which will be completed to handle frequency-domain or parametric robustness specifications. This heuristic approach is very interesting when the control law designer wants to:

- take into account a first controller based on a priori know-how and physical considerations,
- access to modern optimal control framework to manage frequency-domain robustness specifications and the trade-offs between these various specifications.

A multi-objective control design procedure based on the CSF is proposed in [5] and illustrated on a academic mixed-sensibility (2 channels) control problem. Realistic applications of this approach in the field of Aeronautics (Flight control law design) are described in [2] and [4] and, in this chapter, in launch vehicle control design.

Bibliography

[1] D. Alazard. Extracting physical tuning potentiometers from a complex control law: application to flexible aircraft flight control. In *AIAA, Guidance, Navigation and Control Conference*, August 2001.

[2] D. Alazard. Robust H_2 design for lateral flight control of a highly flexible aircraft. *Journal of Guidance, Control and Dynamics*, 25, No. 3:502–509, 2002.

[3] D. Alazard and P. Apkarian. Exact observer-based structures for arbitrary compensators. *International Journal of Robust and Non-Linear Control*, 9:101–118, 1999.

[4] D. Alazard, C. Cumer, and F. Delmond. Improving flight control laws for load alleviation. In *Proceedings of the ASCC2006,* 6^{th} *Asian Control Conference*, Bali (Indonesia), July 2006.

[5] D. Alazard, O. Voinot, and P. Apkarian. A new approach to multiobjective control design from the viewpoint of the inverse optimal control problem. In *Proceedings of the SSSC'04, IFAC Symposium on Systems Structure and Control*, Oaxaca (Mexico), December 2004.

[6] M. Athans. A tutorial on the lqg/ltr method. In *Proc. of American Control Conference*, pages 1289–1296, Seattle (WA), 1986. IEEE.

[7] D. J. Bender and R. A. Fowell. Computing the estimator-controller form of a compensator. *Int. J. Contr.*, 41:1565–1575, 1985.

[8] D. J. Bender, R. A. Fowell, and A. F. Assal. Estimating the plant state from the compensator state. *IEEE Trans. Automat. Contr.*, 31:964–967, 1986.

[9] S. Boyd and L. Vanderberghe. *Convex optimization.* Cambridge University Press, 2003.

[10] C. Cumer, F. Delmond, D. Alazard, and C. Chiappa. Tuning of observer-based controllers. *Journal of Guidance, Control and Dynamics*, 27, No. 4:607–615, 2004.

[11] F. Delmond, D. Alazard, and C. Cumer. Cross standard form: a solution to improve a given controller with h_2 and h_∞ specifications. *International Journal of Control*, 79, No. 4:279–287, 2006.

[12] J. C. Doyle, K. Glover, P. D. Khargonekar, and B. A. Francis. State space solutions to standard $\mathcal{H}_2$ and $\mathcal{H}_\infty$ control problem. *IEEE Transactions on Automatic Control*, 1989.

[13] T. Fujii. A new approach to the LQ design from the viewpoint of the inverse regulator problem. *IEEE. Transactions on Automatic Control*, vol. AC32., No. 11.:995–1004, 1987.

[14] T. Fujii and P.P. Khargonekar. Inverse problems in $\mathcal{H}_\infty$ control thery and linear-quadratic differential games. In *Proceedings of the 27th Conference on Decision and Control*, pages 26–31, Austin (Texas), december 1988. IEEE.

[15] G. H. Golub and C. F. van Loan. *Matrix - Computations*. Studies in the mathematical sciences, J. Hopkins University Press., 1996.

[16] N. Imbert. Robustness analysis of a launcher attitude controller via μ-analysis. In *15th IFAC Symposium on Automatic Control in Aerospace*, Bologna, 2-7 September 2001.

[17] P. P. Khargonekar K. E. Lenz and J. C. Doyle. When is a controller $\mathcal{H}_\infty$ optimal? *Mathematics of Control, Signals and Systems*, 1:107–122, 1988.

[18] J. C. Doyle K. Zhou and K. Glover. *Robust and optimal control*. Prentice Hall, 1996.

[19] R.E. Kalman. When is a linear control optimal? *Transactions of the ASME, Journal of Basic Engineering*, pages 51–60, 1964.

[20] I. Kaminer, A. M. Pascoal, P. P. Khargonekar, and E. E. Coleman. A velocity algorithm for the implementation of gain-scheduled controllers. *Automatica*, 31(8):1185–1191, 1995.

[21] D. A. Lawrence and W. J. Rugh. Gain scheduling dynamic linear controllers for a nonlinear plant. *Automatica*, 31(3):381–290, 1995.

[22] C. F. Van Loan. Computing integrals involving the matrix exponential. *IEEE Transactions on Automatic Control*, AC-23(3):395–404, 1978.

[23] D. G. Luenberger. An introduction to observers. *IEEE Trans. Automat. Contr.*, AC-16:596–602, 1871.

[24] B. P. Molinari. The stable regulator problem and its inverse. *IEEE Trans. on Automatic Control*, vol. AC-18., No. 5.:454–459, 1973.

[25] N. Narasimha-murthi and F. F. Wu. On the riccati equation arising from the study of singularly perturbed systems. *IEEE Joint Automatic Control Conference*, 1977.

[26] P. C. Pellanda, P. Apkarian, and D. Alazard. Gain-scheduling through continuation of observer-based realizations - applications to $\mathcal{H}_\infty$ and μ controllers. In *Proc. 39th IEEE Conf. on Decision and Control*, pages 2787–2792, Sydney, 12-15 December 2000. IEEE.

[27] N. Sebe. A characterization of solutions to the inverse $\mathcal{H}_\infty$ optimal control problem. In *Proceedings of the 40th Conference on Decision and Control*, pages 273–278, Orlando (Florida), december 2001. IEEE.

[28] T. Shimomura and T. Fujii. Strictly positive real $\mathcal{H}_2$ controller synthesis from the viewpoint of the inverse problem. In *Proceedings of the 36th Conference on Decision and Control*, pages 1014–1019, San Diego (California), december 1997. IEEE.

[29] D. J. Stilwell and W. Rugh. Interpolation of observer state feedback controllers for gain scheduling. *IEEE Trans. Automatic Control*, 44(6):1225–1229, 1999.

[30] K. Sugimoto. Partial pole-placement by LQ regulator: An inverse problem approach. *IEEE. Transactions on Automatic Control*, vol. 43., No. 5.:706–708, 1998.

[31] K. Sugimoto and Y. Yamamoto. New solution to the inverse regulator problem by the polynomial matrix method. *International Journal of Control*, 45-5:1627–1640, 1987.

[32] S. Tarbouriech and G. Garcia. Control of uncertain systems with bounded inputs. *Springer Verlag - Lectures notes in control and information sciences*, 1997.

[33] O. Voinot, D. Alazard, A. Piquereau, and A. Biard. A robust multi-objective synthesis applied to launcher attitude control. In *15th IFAC Symposium on Automatic Control in Aerospace*, Bologna, 2-7 September 2001.

[34] O. Voinot, D.Alazard, P. Apkarian, S. Mauffrey, and B. Clment. Launcher attitude control: Discrete-time robust design and gain-scheduling. *IFAC Control Engineering Practice*, 11:1243–1252, 2003.

[35] K. Zhou. Comparison between $\mathcal{H}_2$ and $\mathcal{H}_\infty$ controllers. *IEEE Transaction on Automatic Control*, Vol. 37, No. 8:1261–1265, 1992.

[36] K. Zhou, J. C. Doyle, and K. Glover. *Robust and optimal control*. Prentice Hall, 1996.

Contents